



OPEN ACCESS

EDITED BY

Ángel Puga-Bernabéu,
University of Granada, Spain

REVIEWED BY

Yumao Pang,
Shandong University of Science and
Technology, China
Numair Siddiqui,
University of Technology Petronas, Malaysia

*CORRESPONDENCE

Dandan Hu,
✉ hdd_0619@163.com

RECEIVED 22 September 2023

ACCEPTED 07 February 2024

PUBLISHED 26 February 2024

CITATION

Li W, Hu D, Chang Y, Li Y, Guo B, Shi Q and
Zhang B (2024), Diagenetic controls over
reservoir quality of tight sandstone in the
lower Jurassic reservoir in the Lenghu area,
the north margin of Qaidam basin.
Front. Earth Sci. 12:1298802.
doi: 10.3389/feart.2024.1298802

COPYRIGHT

© 2024 Li, Hu, Chang, Li, Guo, Shi and Zhang.
This is an open-access article distributed
under the terms of the [Creative Commons
Attribution License \(CC BY\)](https://creativecommons.org/licenses/by/4.0/). The use,
distribution or reproduction in other forums is
permitted, provided the original author(s) and
the copyright owner(s) are credited and that
the original publication in this journal is cited,
in accordance with accepted academic
practice. No use, distribution or reproduction
is permitted which does not comply with
these terms.

Diagenetic controls over reservoir quality of tight sandstone in the lower Jurassic reservoir in the Lenghu area, the north margin of Qaidam basin

Wenhuan Li¹, Dandan Hu^{1*}, Yuwen Chang¹, Ya'nan Li²,
Bin Guo³, Qi Shi² and Bin Zhang⁴

¹Research Institute of Petroleum Exploration and Development PetroChina, Beijing, China, ²Research Institute of Exploration and Development of Qinghai Oilfield Company, PetroChina, Dunhuang, China, ³New Energy Department of Qinghai Oilfield Company, PetroChina, Dunhuang, China, ⁴Research Institute of Petroleum Exploration and Development, Zhongyuan Oilfield Company, China Petroleum & Chemical Corporation, Puyang, China

The Lower Jurassic Reservoir (LJR) in the Lenghu area on the northern margin of the Qaidam Basin (NMoQB) has become the most promising target for hydrocarbon exploration. The reservoir has experienced complex diagenesis; however, the porosity evolution and the influence of different diagenesis events on reservoir densification remains unclear. In this study, various analytical methods were first used to clarify the diagenetic stage and sequence, establish a porosity evolution model, quantitatively analyze the time and influence of different diagenesis events on reservoir densification, and illustrate the densification mechanism of tight sandstone reservoir in the Lenghu area. The results showed that the dominant rock types in the LJR were feldspathic litharenite, followed by litharenite, lithic arkose, and a small amount of subarkose and sublitharenite. The reservoir is a typical tight sandstone reservoir (TSR), with average porosity and permeability of 5.5% and 0.08 mD, respectively. The pore types were primarily secondary pores, followed by residual intergranular pores and occasional fractures. Diagenesis of LJR has entered the meso-diagenetic stage A, with minor progression into meso-diagenetic stage B. Quantitative calculation showed that the initial porosity of LJR is 32.2%. In eo-diagenetic stage A, compaction is the main factor for porosity reduction. In eo-diagenetic stage B, the porosity loss rates caused by compaction and cementation were 81.5% and 11.8%, respectively. In this stage, the LJR in the Lenghu area has almost been densified, mainly affected by compaction, calcite cementation and clay minerals cementation. Additionally, cementation is an important factor causing reservoir heterogeneity and is dominated by calcite and clay mineral cementation. After entering the meso-diagenetic stage A, dissolution is the main diagenesis event, which can increase porosity by 6.0%. This stage is the critical period for forming high-quality reservoir of LJR in the Lenghu area, mainly in the 4,400 m depth. In meso-diagenetic stage B, the influence of

dissolution gradually decreased. Simultaneously, in this stage, the cementation of iron-bearing calcite further strengthened the densification of the LJR in the Lenghu area.

KEYWORDS

diagenesis, pore evolution, reservoir quality, tight sandstone reservoirs, Lenghu area, the north margin of Qaidam basin

1 Introduction

With the increasing difficulty in traditional oil and gas development, unconventional resources (shale oil, tight oil, etc.) have gradually become important hydrocarbon resources (Law and Curtis, 2002; Zou et al., 2010; Dai et al., 2012; Jia, 2017; Ju and Wang, 2018; Liu et al., 2022; Qin et al., 2022; Liu et al., 2023). Tight oil has become a significant contender for replacing traditional energy resources and supporting the ongoing industrial revolution. Tight oil is generally defined as oil flow in tight reservoirs with permeability ≤ 0.1 mD (Zou et al., 2012; Sun et al., 2019; Fang et al., 2020). Approximately 66 tight oil basins exist worldwide. Currently, China has many tight oil-scale reserves in Ordos, Sichuan, Songliao, Junggar, Bohai Bay, and the Qaidam Basin (Zhu et al., 2018; Sun et al., 2019; Wu et al., 2022). By the end of 2022, the geological reserves of tight oil in China were 133.7×10^8 t, accounting for 6.3% of the total oil geological reserves, with excellent exploration potential (Wu et al., 2022).

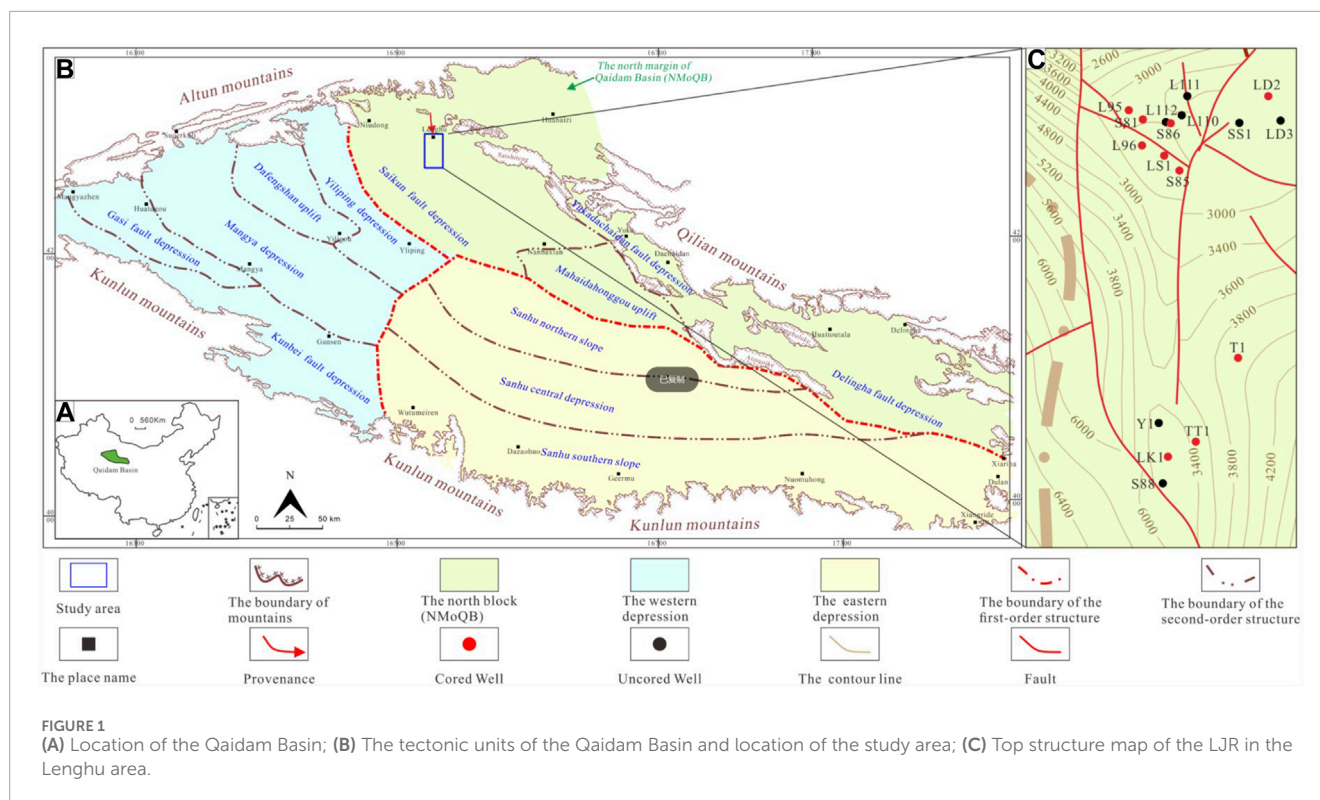
Compared with conventional reservoirs, tight sandstone reservoirs often undergo complex burial processes and strong diagenetic transformation. They have the characteristics of complex reservoir space, narrow pore throat radius, nanoscale pore throat system development, and strong reservoir heterogeneity (Karim et al., 2010; Xi et al., 2015; Wang et al., 2019; Liu et al., 2022; Xu et al., 2022). In the formation process of tight sandstone reservoirs, densification is often a complex process of multiple diagenetic events, and there are significant differences in different stages and locations (Zhang et al., 2014; Su et al., 2021; Zhu et al., 2022). For tight sandstone reservoirs, the study of pore evolution process and reservoir densification mechanism is a hot spot of current research, which can provide a theoretical basis and practical guidance for the efficient exploration and development of tight sandstone reservoirs (Yuan et al., 2015; Su et al., 2021; Zhu et al., 2022; Xiao et al., 2023).

Predecessors have carried out a lot of research on the densification mechanism of different tight sandstone reservoirs, and the reservoirs densification mechanism in different petroliferous basins are controlled by different diagenetic events (Zhang, 2008; Liu et al., 2011; Guo et al., 2012; Zhuo et al., 2015; Lai et al., 2016; Wang et al., 2020; Dai et al., 2021). Now, it can be divided into four categories: a) In low-energy or turbidite sedimentary environments, the matrix content between clastic particles is high, thus forming argillaceous sandstone. Simultaneously, a large amount of mud and matrix fills the intergranular pores, and the pores in the reservoir are almost all micropores, and the reservoir densification is serious; b) In the process of burial, the sandstone with high plastic content is easily compacted under the overlying formation pressure, forming a tight sandstone reservoir; c) During diagenesis, various types of

cements precipitated and fill reservoir spaces, such as intergranular pores and dissolved pores, forming tight sandstone reservoirs; d) During the diagenetic process, authigenic clay minerals precipitated, filling the reservoir space or plugging the pore throat, forming tight sandstone reservoirs.

Previous studies on the densification mechanism of tight sandstone reservoirs have primarily focused on qualitatively analyzing the influence of various factors, such as sedimentation, diagenesis, and tectonism, on reservoir properties (Li et al., 2017a; Wu et al., 2019; Cao et al., 2020). However, the stage and controlling factors of reservoir densification remain unclear. To gain a comprehensive and objective understanding of the reservoir densification mechanism, it is crucial to quantitatively analyze the types of diagenetic events occurring in each stage and their contribution to reservoir densification, thus clarifying the determinants and time of reservoir densification formation and illuminating the mechanism.

In recent years, owing to the continuous discovery of industrial oil and gas flows, the northern margin of the Qaidam Basin (NMoQB) has become a popular research area (Ma et al., 2018; Tian et al., 2022). However, the extensive development of TSR has become a key factor limiting further exploration and development of oil and gas reservoirs in the NMoQB. The Lower Jurassic Reservoir (LJR) in the Lenghu area of the NMoQB is a typical TSR (Zhao et al., 2020). The development of the Lenghu IV-V oil fields indicates that this area has high exploration prospects. Predecessors have done a lot of research on the Lenghu area. Xu et al. (2008) believed that hydrocarbon source rocks of the Lower Jurassic Formation in the Lenghu area are mainly low-mature, and some areas have entered a high-mature stage. Guo (Guo et al., 2017) studied the sedimentary diagenesis environment in this area, and clarified that at the early stage of the LJR had a warm and humid climate, dominated by fresh water deposition, and the late climate was gradually dry and hot, dominated by fresh water-brackish water. Sun (Sun et al., 2012) pointed out that the Lenghu area is a fault block uplift in the hydrocarbon generating depression, which is dominated by structural combination oil and gas reservoirs. Through the relationship between structural distribution and reservoir accumulation, Ma (Ma et al., 2018) concluded that the structure controlled the distribution of Jurassic hydrocarbon source rocks in this area, and the fault was the main channel for hydrocarbon migration. Previous studies on Lower Jurassic formation in the Lenghu area mainly focused on geochemistry, structure and oil and gas accumulation, but few research on reservoir. And various unfavorable factors, including deep burial depth, strong denudation, poor seismic quality, and shortage of drilling data further limited our understanding of LJR in the Lenghu area, leaving gaps in our understanding of the diagenesis characteristics, porosity evolution, and the influence of different



diagenesis events on reservoir densification. These factors remain unclear, highlighting the need for further research (He et al., 2021).

Therefore, the purpose of this study is to analyse the types and characteristics of different diagenetic events in each diagenetic evolution stage, quantitatively analyse their contribution to reservoir densification, clarify the stage and main controlling factors of tight sandstone reservoir formation in the Lenghu area, and clarify its densification mechanism, so as to provide a theoretical basis for the next exploration and development in this area. For the analysis, we employed a range of techniques, including core observation, physical properties, cast thin section (CTS), grain size analysis, scanning electron microscopy (SEM), X-ray diffraction (XRD) analysis, and vitrinite reflectance (R_o). The specific research objects were as follows:

1) To clarify the petrological characteristics, petrophysical properties, and pore types of the LJR; 2) to investigate the diagenetic characteristics and diagenetic paragenetic sequence; 3) to establish a porosity evolution mode and quantitatively analyse the time and influence of different diagenesis events on reservoir densification; 4) to illustrate the densification mechanism of tight sandstone reservoir in the Lenghu area. This study provides solid theoretical guidance for further exploration and development in this area as well as new insights for the research of similar TSRs.

2 Geological setting

Located on the northeastern Qinghai-Tibet Plateau, the Qaidam Basin is an inland intermountain basin with a total area of $12 \times 10^4 \text{ km}^2$ (Figure 1A). It is a large Mesozoic and Cenozoic petroliferous basin located in northwestern China (Zhao et al., 2020;

Li et al., 2021; Zhang et al., 2022). The Basin is diamond-shaped (Mao et al., 2016; Guo et al., 2019). The north is bounded by the Qilian mountains, the west by the Altun strike-slip fault, and the south by the Kunlun mountains (Tian et al., 2018; Guo et al., 2022; Hou et al., 2022). The entire basin is composed of three tectonic units: the northern fault block (NMoQB), the western depression, and the eastern depression (Fu et al., 2013). NMoQB is located in the northwest of the basin, with an area of $3.34 \times 10^4 \text{ km}^2$. It is composed of three secondary structural units (Saikun fault depression, Delingha fault depression, and Mahaidahonggou uplift) (Figure 1B) (Tian et al., 2018). The Qaidam Block has undergone multiple tectonic movements, including Caledonian, Hercynian, Indosinian, Yanshan and Himalayan, forming the Qaidam Basin—a composite inland sedimentary basin (Zhang et al., 2009; Cao et al., 2018). Its tectonic evolution can be divided into three stages: a) Pre-Sinian crystalline basement tectonic evolution stage; b) Sinian-Triassic tectonic evolution stage, and c) Meso-Cenozoic tectonic evolution stage of an inland lake basin (Tang et al., 2000).

Mesozoic strata (mainly Jurassic and Cretaceous) are widely developed in the NMoQB. From bottom to top, the Jurassic strata successively developed Xiaomeigou Formation (J_{1x}), Dameigou Formation (J_{2d}), Caishiling Formation (J_{31c}), and Hongshuigou Formation (J_{32h}). While the Cretaceous only developed the Quanyagou formation (K_1). As for the Cenozoic strata, the Lulehe Formation (E_{1+2}), Xiaganchaigou formation (consist of Lower member of Xiaganchaigou Formation (E_3^1) and Upper member of Xiaganchaigou Formation (E_3^2)), Shanggancaigou Formation (N_1), Youshashan Formation (consist of Lower Youshashan Formation (N_2^1) and Upper Youshashan Formation (N_2^2)), Shizigou

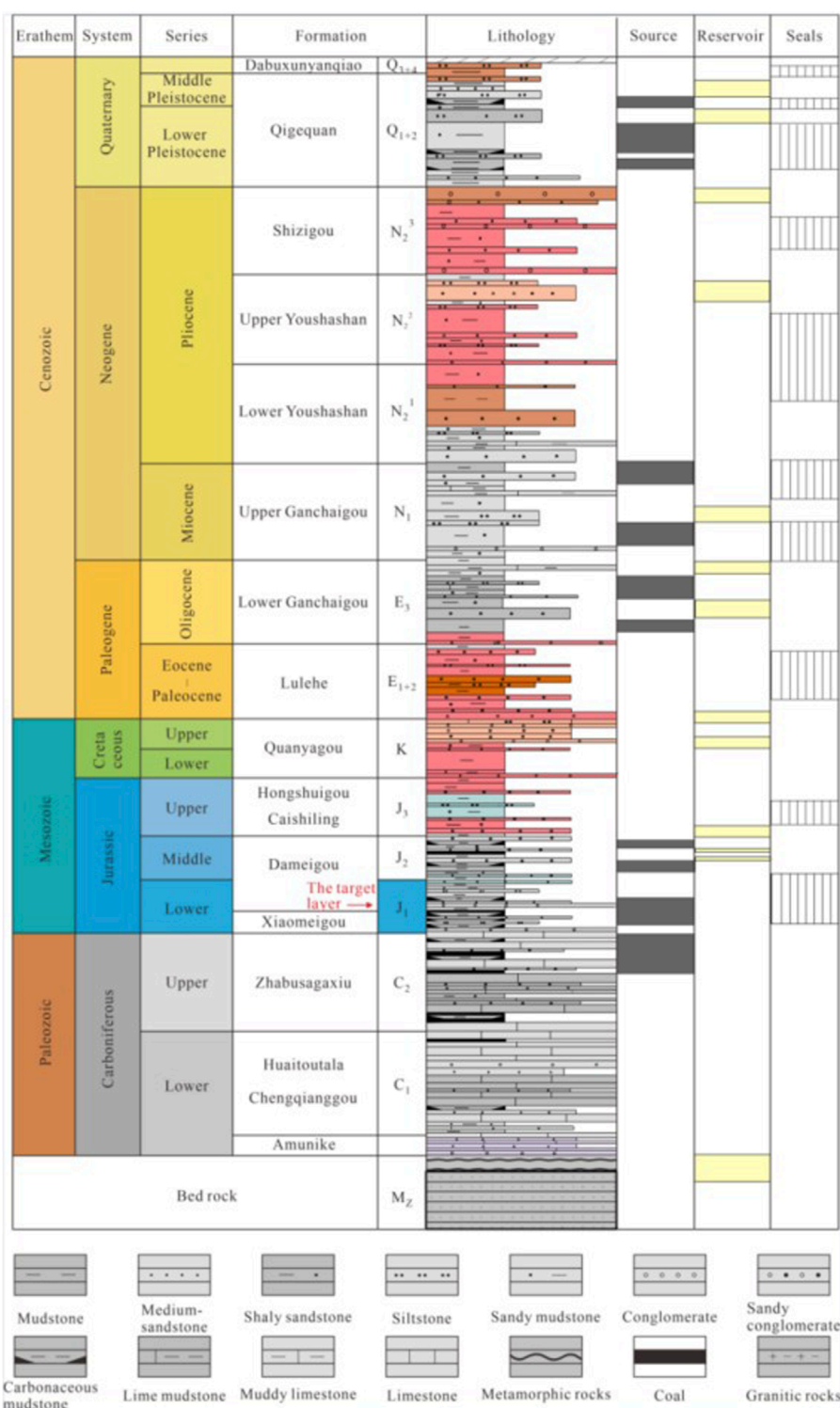
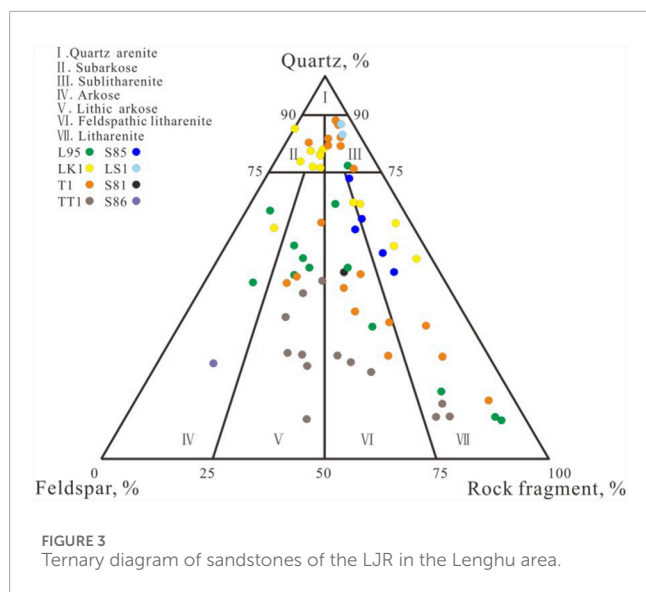


FIGURE 2 The stratigraphic column of Paleozoic-Mesozoic-Cenozoic in the Qaidam Basin.

Formation (N₂³) and Qigequan Formation (Q₁₊₂) were continuously deposited from old to new (Figure 2; Tian et al., 2022).

The Lenghu area belongs to a secondary antinormal structure of the Saikun fault depression in the NMOQB (Figures 1B,C). Under the

influence of source rock and two tectonic movements (the Yanshan movement and the Himalayan movement), the Lenghu area has become a favorable location for oil and gas accumulation. And it was also one of the earliest discovered areas of the industrial oil



flow in the basin (Zhang et al., 2009; Tian et al., 2018; Zhao et al., 2020; He et al., 2021). Jurassic, Paleogene, and Neogene strata are developed from bottom to top in the Lenghu area, with the middle and lower Jurassic mudstone serving as the source rock (Sun et al., 2006; Xu et al., 2008). In addition, the LJR reservoir in this area is the key exploratory stratum of the NMoQB.

The provenance of the Lenghu area comes from the piedmont of the Xiaosaishiteng Mountain (Liu et al., 2022). From the piedmont to the study area, alluvial fan-nearshore subaqueous fan-lake developed in turn, forming a complete sedimentary system from the edge to the center of the lake basin. The LJR in the study area develops nearshore subaqueous fan and sublacustrine fan systems (Sun et al., 2006; Zou et al., 2012). The rock types are mainly dark lacustrine mudstone, carbonaceous mudstone, and gray siltstone interbedded with coal bearing source rocks (Ritts et al., 1999; Zhai et al., 2013; Tian et al., 2018; Han et al., 2020).

3 Methods and materials

In this study, the LJR samples were obtained from 10 wells. Additionally, 69 grain-size analyses of six wells, 32 Rock-Eval pyrolysis data from four wells, and 27 XRD data from three wells were obtained from the Qinghai Oilfield Exploration and Development Research Institute. Overall, 85 samples were used for porosity and permeability measurements. These samples were drilled from six wells and shaped into small cylinders 2.5 cm in diameter. The ultra-Pore 400 porosity tester and a DX-07G permeability tester were used to measure porosity and permeability, respectively. Thirty-five cast thin sections were prepared to count the number of clastic particles and carbonate cement particles. Each thin section contained 350 points. All slices were stained with alizarin red, calcite was stained red, iron calcite was stained purple, dolomite was not stained, and iron dolomite was stained blue. The Ro of the 13 mudstone samples was using a highly precise MPM600 microphotometer. To ensure the accuracy of the data, each sample was effectively measured ten times, and the average value

was obtained. SEM was used to identify the type and morphology of authigenic minerals, diagenesis, and pore structure characteristics. In this study, 78 samples from seven wells were used to prepare gold-plated slices for SEM analysis. These slices were observed using a Zeiss-18 scanning electron microscope.

4 Results

4.1 Petrological characteristics

Based on the thin-section observation results, the rock-types of the LJR are diverse. According to the classification of sandstones proposed by Folk (1980), they are dominated mainly by feldspathic litharenite, followed by litharenite and lithic arkose, small amounts of subarkose and sublitharenite, and occasionally arkose (Figure 3). Quartz ranges from 10.11% to 88.51% (avg. 52.63%). Rock fragments varied greatly (0.00–84.27%), with an average of 28.48%. Feldspar is between 2.78% and 62.50% (avg. 18.89%). The lithic components are dominated by metamorphic grains with small amounts of volcanic lithics. The particles are characterized by line and point-line contact, well to medium sorting, and subangular roundness. The cementation between the particles is dominated by pore cementation, with a lesser extent of embedded cementation.

4.2 Pore types

CTS and SEM observations indicated that the pores of the LJR are dominated by secondary pores, with some residual intergranular pores (Figures 4A,C–E) and occasional fractures. Secondary pores are composed of intergranular and intragranular dissolution pores. Thin-section analysis indicates that the pores in the Lenghu area mostly existed in the form of a combination, and samples with intergranular dissolved pores and intragranular dissolved pores are mainly developed (Figure 4B). The characteristics of different pore types are introduced as follows:

The intergranular pores formed by the dissolution of primary intergranular pores around feldspar, quartz, and other grains. The pore size is uneven and the shape is bay-like or irregular (Figure 4A). Intragranular dissolved pores are often distributed in the interior of easily soluble particles such as feldspar and rock fragments, with honeycomb or point-like structures (Figures 4B–D,F). Mould pores formed when the particles dissolved. Furthermore, due to overlying pressure and tectonic movement, few fractures can be observed in thin sections (Figure 4F).

4.3 Porosity and permeability

Based on the results of approximately 85 sandstone samples of reservoir property data from the study area, the porosity of the sandstones ranges from 0.3% to 14.3% (avg. 5.5%). According to the reservoir classification standard of China (SY/T6285-2011), the porosity was dominated by ultra-low porosity (42.3%), followed by extra-low porosity (40.0%) (Figure 5A); Permeability varies between 0.01 and 13.17 mD (avg. 0.08 mD) (Figure 5B). It is dominated by ultra-low permeability, accounting for more than 86.9%.

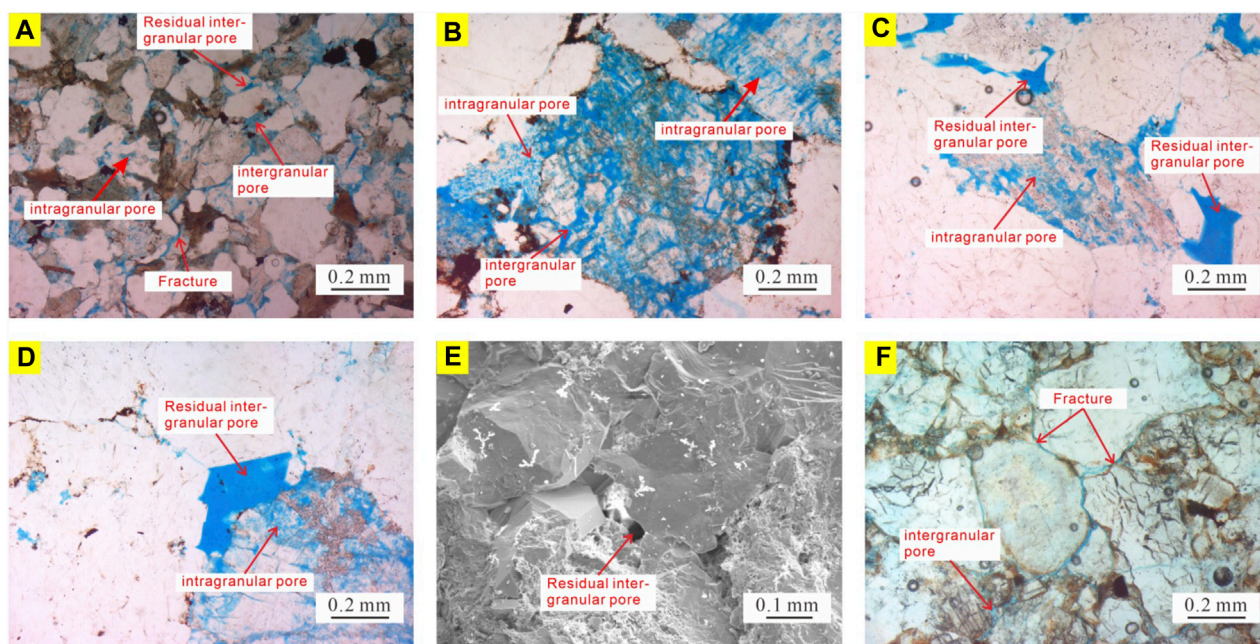


FIGURE 4 Pore types of the LJR in the Lenghu area: (A) residual intergranular pore, intergranular pore, intragranular pore, fracture (L95, 3357.89 m); (B) intergranular and intragranular pores (LK1, 4317.91 m); (C) intragranular pore, residual intergranular pore (LK1, 4315.56 m); (D) intragranular pore, residual intergranular pore (LK1, 4317.91 m); (E) residual intergranular pore (LK1, 4315.56 m); (F) intergranular pore, fracture (S81, 3204.00 m).

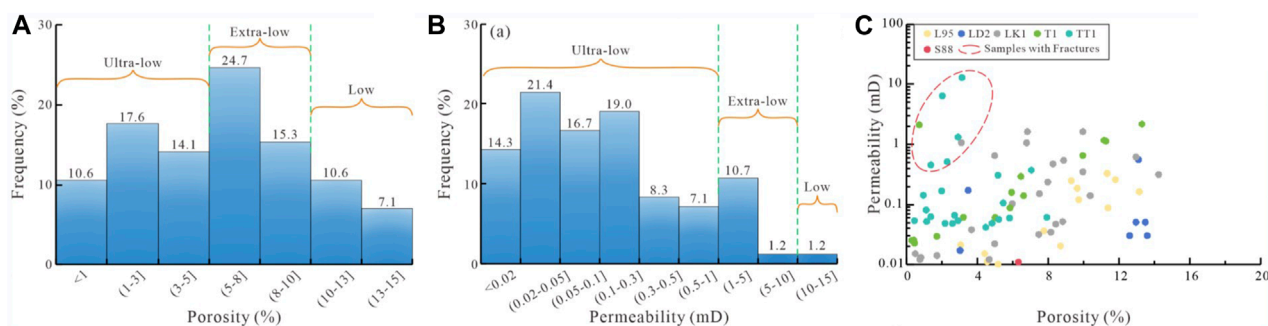


FIGURE 5 Physical properties of the LJR in the Lenghu area: frequency distribution histogram of (A) porosity and (B) permeability, (C) the crossplots of porosity and permeability.

The correlation between porosity and permeability is complex. Figure 5 shows that the physical properties of most coring well samples have a large span and show strong heterogeneity (Figure 5C). In addition, some samples had a low porosity, but the corresponding permeability was high, indicating the development of fractures. Some samples have high porosity, but the related permeability was very low, meaning poor pore structure (Figure 5C).

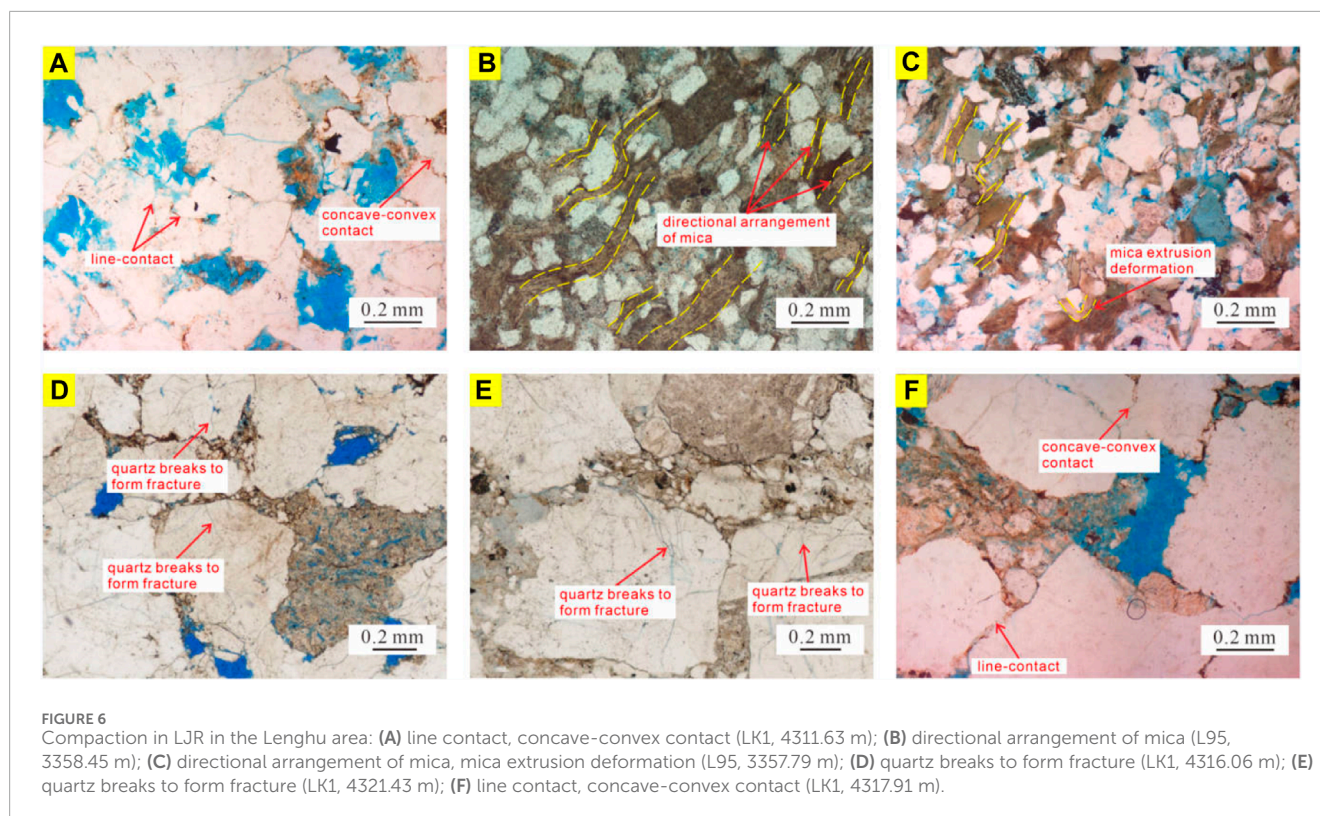
4.4 Diagenesis

Diagenesis is a crucial factor that affects the reservoir quality. Based on the CTS and SEM observations, the diagenesis of LJR

mainly consisted of mechanical compaction, chemical compaction, cementation, and dissolution, as discussed below.

4.4.1 Compaction

The LJR in the study area was deeply buried; the maximum buried depth was 5,200 m and the compaction intensity was high. The CTS analyses revealed four compaction types (Figure 6): a) particles were mainly in line and point-line contact (Figure 6A); b) due to the pressure of the overlying formation, plastic particles (such as mica) appeared in a directional arrangement (Figures 6B,C) or extrusion deformation (Figure 6C); c) rigid particles (feldspar, quartz, etc.) deformed or broke under the influence of the overlying pressure (Figures 6D,E); d) Chemical pressure solution is observed



and some particles are in concave-convex contacts, and a stylolite structure could be observed (Figures 6A,F).

4.4.2 Dissolution

Dissolution can effectively improve the reservoir properties and is prevalent in the Lenghu area. CTS observations show that the dissolution characteristics of the LJR can be divided into four groups: a) the edge of soluble particles (feldspar, rock fragment, etc.) was dissolved, forming bay-like or irregular intergranular dissolution pores (Figure 7A); b) the interior of the particles (feldspar, rock fragment and calcite, etc.) was dissolved by acidic fluid, forming point-like or honeycomb-like intragranular dissolution pores (Figures 7B–D); c) feldspar or quartz grains were dissolved along their cleavage fractures (this type of dissolution can effectively improve reservoir permeability) (Figure 7E); and d) strong dissolution caused the particles to completely dissolve and led to the formation of mould pore (Figure 7F).

4.4.3 Cementation

According to the CTS analyses and SEM observations, Cements in the LJR are predominantly composed of carbonate, clay, and a small amount of siliceous cement.

4.4.3.1 Carbonate cementation

Carbonate is the most common cement type found in the TSR (Zhu et al., 2019). In the Lenghu area, carbonate cementation is dominated by calcite, which can be observed in more than 60% of the thin sections. Based on the CTS observations, three different phases of calcite cement were identified: a) the first phase of calcite cementation occurred in the eo-diagenesis stage. Under the observation of cast thin sections, the crystal morphology of

early calcite cement usually presents small particles, which are hexagonal or prismatic. And the connectivity between crystals is relatively poor (Figure 8A); b) the second phase of calcite developed among the skeleton particles in the form of crystals, and its content was relatively high. This type of calcite was formed in the meso-diagenetic stage A (Figure 8B); c) The third phase of calcite formed in the meso-diagenetic stage B and was characterized by the development of iron-bearing calcite, distributed in dissolution pores (Figure 8C).

4.4.3.2 Clay mineral cementation

The SEM and XRD results showed the development of various types of clay minerals, including kaolinite, illite, I/S (illite/smectite) mixed layer, and smectite. Among these, the kaolinite content was relatively high, followed by the I/S mixed layer and illite. Chlorite is relatively scarce, and smectite is occasionally observed. Smectite is found only at a depth of around 3350 m; The I/S mixed layer, illite, and kaolinite contents are relatively high at 4,150 m and 4,320 m depths; The chlorite content is higher at 3,350 m, which gradually decreases with the increase in depth (Figure 9). The morphology of the kaolinite crystals is well-developed. Single kaolinite crystals are pseudo-hexagonal, plate-like, and the aggregates have a book-like structure. This type of kaolinite is generally formed by direct precipitation in the pore fluid or gradual evolution from the early smaller kaolinite. Kaolinite is often observed in the intergranular or dissolution pores (Figure 8D). Illite is filamentous or flaky with bridging or pore filling between the particles (Figures 8E,F). The I/S mixed layer mainly developed in pores with a curled shape (Figure 8G). Chlorite is relatively scarce in the study area, predominantly present as a chlorite film growing vertically along the surfaces of clastic particles (Figure 8H).

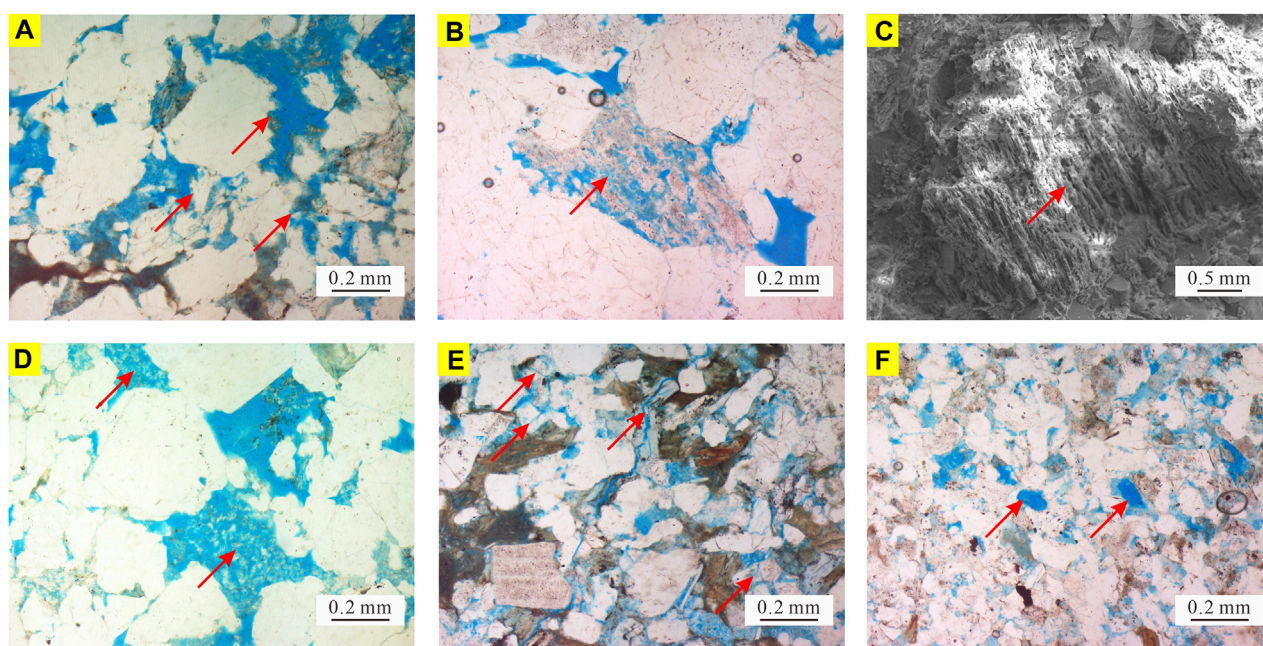


FIGURE 7
Dissolution of the LJR in the Lenghu area: (A) intergranular dissolution pores (LK1, 3483.75 m); (B) intragranular dissolution of feldspar (LK1, 4315.56 m); (C) intragranular dissolution of feldspar (LK1, 3482.25 m); (D) intragranular dissolution of feldspar (LK1, 3482.25 m); (E) particles dissolve along cleavage fractures (L95, 3357.89 m); (F) particles are completely dissolved to form mold pore (LK1, 4314.68 m).

4.4.3.3 Siliceous cementation

Quartz overgrowth was the main siliceous cementation of LJR, and its degree of enlargement was grade II (Figures 8E,I). When observed under an SEM, quartz overgrowth typically appears as a hexagonal crystal shape. The crystal plane is usually flat with a clear planar structure. Additionally, quartz overgrowth shows good reflection, reflecting the fine electron beam and producing a bright image. Quartz overgrowths can occupy part of the intergranular pores, thus reducing the reservoir properties to a certain extent. Quartz overgrowth was relatively undeveloped in the LJR.

4.5 Organic matter maturity

The R_o and Rock-Eval pyrolysis are commonly used to determine the maturity of organic matter. The test results of 13 mudstone samples show that the R_o of LJR is between 0.575 and 0.882 (avg. 0.767) (Supplementary Table S1). Rock-Eval pyrolysis data showed that the organic matter of LJR was mainly mature, and a small part was highly-mature (Supplementary Table S2).

5 Discussion

5.1 Diagenetic stages and sequence

Particle contact, pore type, and authigenic mineral characteristics can generally determine the diagenetic stage. The diagenetic characteristics of the LJR were as follows: a) particles were mainly in line and point-line contact; b) quartz overgrowth

developed, and its degree was predominantly grade II; c) pore types were dominated by secondary pores, followed by some residual intergranular pores and occasionally fractures; d) the clay minerals are dominated by kaolinite and an I/S mixed layer, followed by illite, and a small amount of chlorite. Kaolinite is mainly observed in the form of book-like structures, while, the I/S mixed layer was mostly curved and illite appeared filamentous or flaky; e) the proportion of smectite in the I/S mixed layer is between 5% and 18% (avg. 7.78%); f) R_o is between 0.575 and 0.882 (avg. 0.767) (Supplementary Table S1); g) dissolution developed both in feldspar and rock fragments, with the feldspar dissolution more common; h) the development of dark organic matter indicated that the organic matter in the reservoir has matured; i) Rock-Eval pyrolysis data showed that the organic matter of LJR was mainly mature, and a small part was highly-mature (Supplementary Table S2). All these phenomena suggest that LJR entered meso-diagenesis A, with minor progression into meso-diagenetic stage B.

The diagenetic sequence of the LJR was complex. Based on the CTS and SEM, the paragenetic sequence can be clarified by analyzing the morphology and distribution of authigenic clay minerals at different diagenetic stages. The results are as follows: a) Chlorite film developed vertically on the surface of clastic particles, which indicates that the early compaction occurred earlier than the formation of chlorite film (Figure 10A); b) The first phase of calcite cement could be observed in intergranular pores, and the adjacent particles were surrounded by chlorite film. This suggests that the first phase of calcite cement was formed after the development of the early chlorite film (Figures 10B,C); c) quartz overgrowth often occurs around quartz with no chlorite film, indicating that chlorite had a certain inhibitory effect on

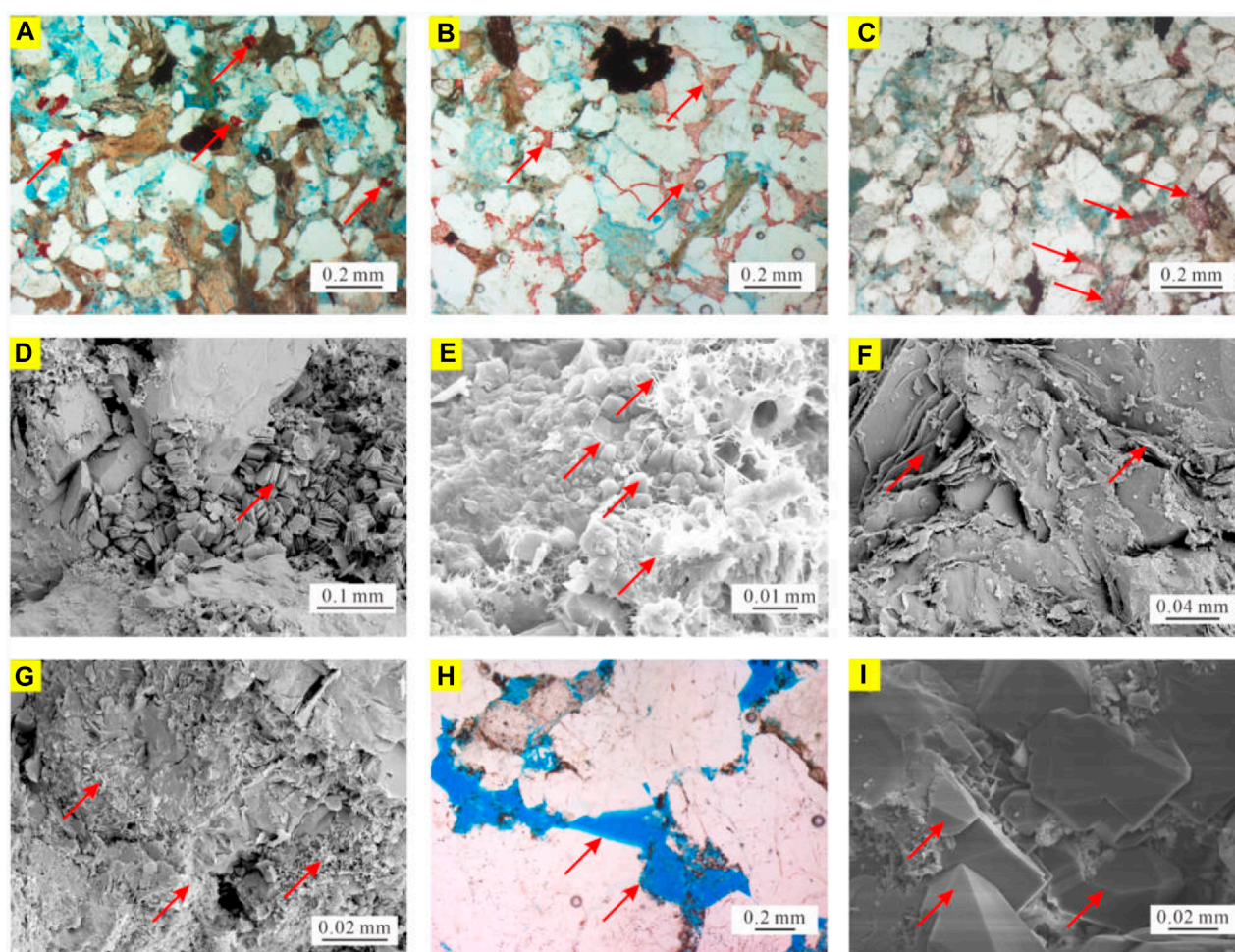


FIGURE 8
Cementsations of the LJR in the Lenghu area: (A) the first phase of calcite cementation (L95, 3357.89 m); (B) the second phase of calcite cementation (LS1, 2832.1 m); (C) iron-bearing calcite filled the intergranular pores (T1, 4435.77 m); (D) book-like kaolinite filling the intergranular pores (LK1, 4316.06 m); (E) quartz overgrowth, filamentous and flaky illite (LK1, 4316.56 m); (F) flaky illite (LK1, 4382.10 m); (G) I/S mixed layer (LK1, 4310.83 m); (H) chlorite film (LK1, 4316.26 m); (I) quartz overgrowth (LK1, 4383.75 m).

quartz overgrowth and that chlorite film formed earlier than quartz overgrowth (Figure 10D); d) clay minerals (book-like kaolinite, filamentous illite, etc.) were observed in the dissolution pores of feldspar, which means they precipitated after the dissolution of feldspar (Figures 10E,F); e) some iron-bearing calcite filled in the intergranular dissolution pores, indicating that the iron-bearing calcite precipitated after dissolution (Figure 10G); f) some dark organic matter developed in dissolution pores, indicating that hydrocarbon charging occurred after dissolution (Figures 10H,I). During the complex diagenetic evolution process, various events occurred alternately and repeatedly.

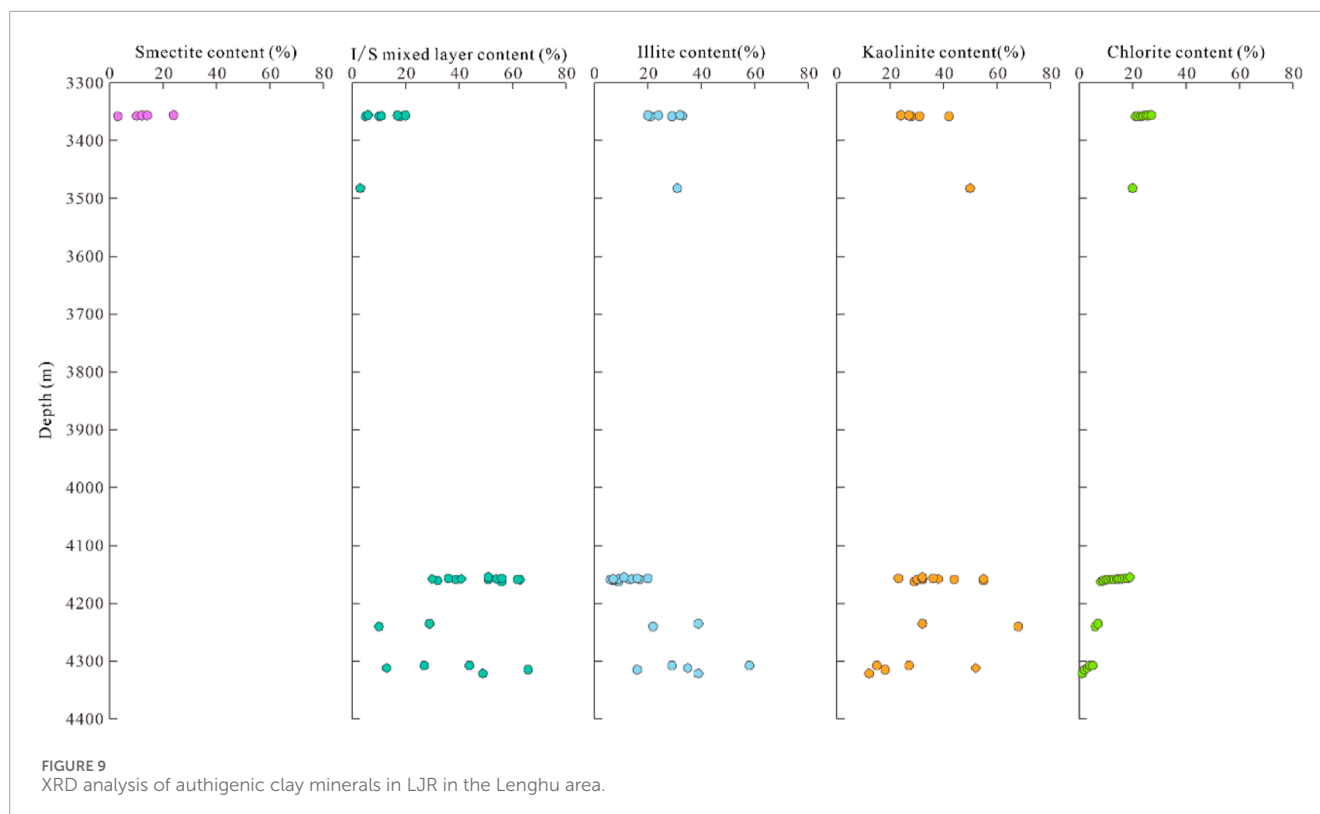
Overall, the paragenetic sequence of LJR in the study area can be reconstructed as follows: Early mechanical compaction → Formation of early chlorite film → Precipitation of early smectite → Cementation of the first phase of calcite → Occurrence of quartz overgrowth → Precipitation of kaolinite → Precipitation of I/S mixed layer → Cementation of second phase calcite → Slight dissolution in feldspar and rock fragment → Precipitation of illite → Dissolution of calcite cement → Hydrocarbon charging → Precipitation

of some iron-bearing calcite → The occurrence of chemical compaction → The occurrence of a small number of fractures (Figure 11).

5.2 Porosity evolution model

Clarifying the porosity evolution is essential for characterizing the densification of the TSR. The initial porosity of the LJR is determined using an empirical formula proposed by Beard and Weyl in the 1970s (Beard and Weyl, 1973). Moreover, thin-section observations were used to quantitatively analyze porosity evolution. The parameters and equations used in this calculation are listed in Supplementary Table S3.

The results of the quantitative analysis indicate that the initial porosity of LJR was 32.2%, which is much lower than the conventional 40% for similar sediments (Houseknecht, 1989; Wang et al., 2020) (Supplementary Table S4). Based on the regional burial history (Zhou et al., 2019; Pang et al., 2022), para-diagenetic



sequence, CTS, and SEM observations, combined with the results of quantitative analysis, this study established an evolution model of the LJR porosity (Figure 12).

In the early burial stage, diagenesis had little influence on reservoir properties. The particles floated, with no contact between them; therefore, the primary intergranular pores were the main pore types. The deeper the burial, the greater the intensity of compaction. The contact between the particles was mainly point contact with a small amount of point-line contact. During this process, mechanical compaction rapidly decreased the reservoir properties. In addition, early cementation had a destructive effect on the reservoir properties. The early chlorite film appeared to have a certain resistance to early compaction. In addition, a small amount of smectite, the first phase of the calcite cement, and quartz overgrowths could also be precipitated (Figure 12).

In the eo-diagenetic stage B, mechanical compaction intensified, leading to the directional arrangement of mica and line and point-line contact between particles. This stage marked the peak impact of mechanical compaction on the reservoir properties. Quantitative analysis results showed a reduction of porosity with residual porosity of 6.0% after compaction, indicating a porosity loss rate of 81.5% during the process. At this stage, slightly acidic fluid dissolved the soluble substances forming intergranular and intragranular dissolution pores. With the evolution of diagenesis, cementation gradually intensified. The second phase of calcite precipitated as crystals among the particles and filled the intergranular pores. Observations indicated kaolinization of feldspar and precipitation of a small amount of kaolinite. In addition, a small amount of illite was observed. As diagenesis continued, a lot of I/S mixed layers

and illite precipitated. And the third phase calcite (iron-bearing calcite) can also be observed. During this stage, cementation had the greatest influence on reservoir properties. According to quantitative analysis results, the loss rate of porosity after cementation was 11.8% (Figure 12).

After entering meso-diagenesis stage A, the mechanical were no longer the main factors affecting reservoir quality. Chemical compaction occurred during this time, and the stylolite structure was observed under the microscope. At this stage, many organic acids were released during the conversion of organic matter to hydrocarbons. The intrusion of acidic fluids caused the dissolution of soluble substances, forming dissolution pores. Dissolution also occurred inside the calcite particles, forming intergranular dissolution pores. In addition, acidic fluids dissolved the cleavage fractures to form microfractures. This stage was dominated by dissolution, which can significantly improve the reservoir properties. According to quantitative calculations, the reservoir porosity increased by 6.0% after dissolution (Figure 12).

In meso-diagenetic stage B, the influence of dissolution gradually decreased, and a small number of fractures were observed. Fractures were relatively undeveloped in the LJR and had little impact on reservoir properties (Figure 12).

Quantitative analysis of porosity evolution has demonstrated that, affected by different diagenesis, the calculated porosity of these analyzed samples was 8.1%, and the measured porosity was 8.2%; the error between them was only 1.3, which fell within the acceptable margin of error (Supplementary Table S4).

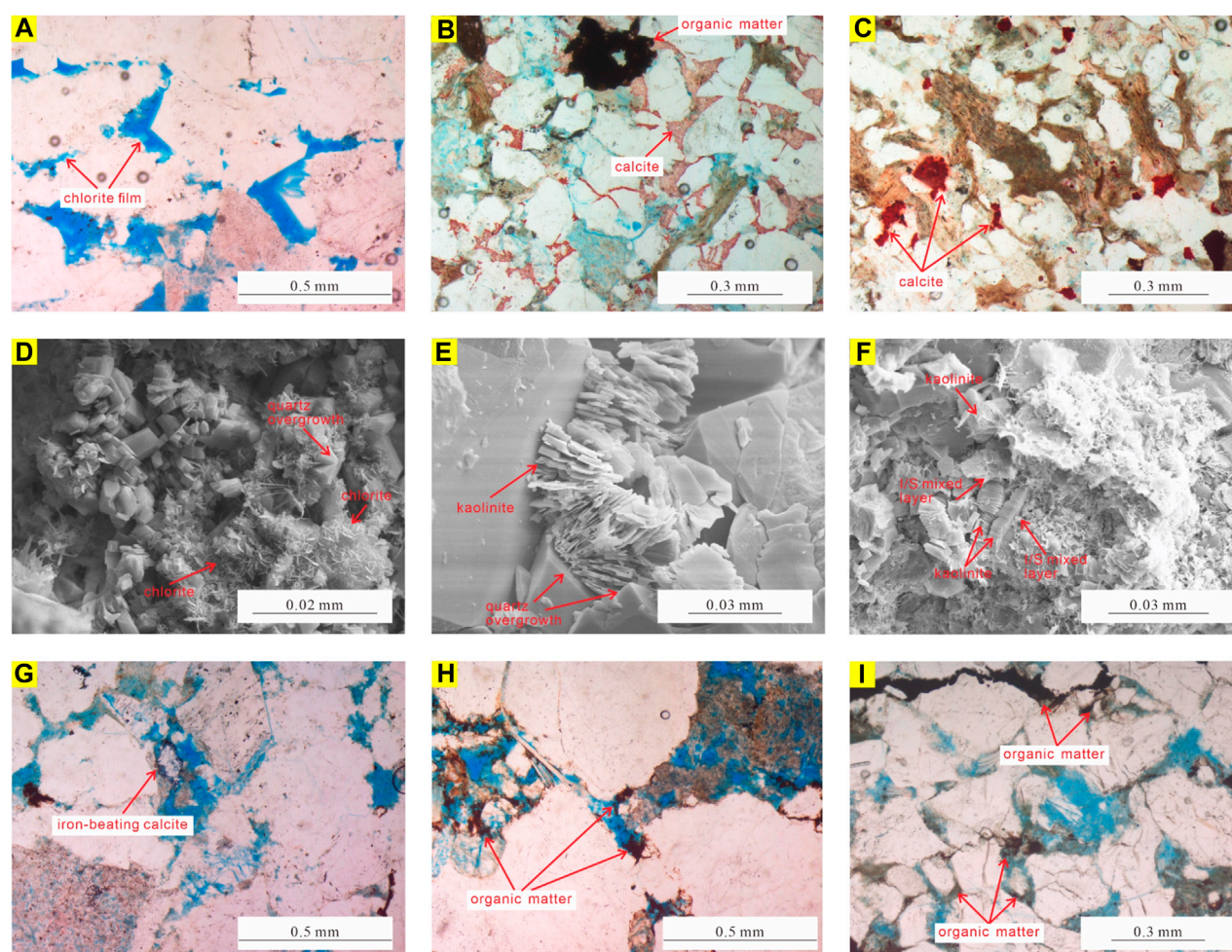


FIGURE 10

Characteristics of paragenetic sequence in LJR in the Lenghu area: (A) chlorite film on the surface of clastic particles (LK1, 4315.56 m); (B) calcite filled the intergranular pores formed by particles which surrounded with chlorite film (LS1, 2832.10 m); (C) calcite filled the intergranular pores formed by particles which surrounded with chlorite film (L95, 3357.89 m); (D) quartz overgrowth occurred around quartz without chlorite film (T1, 4433.64 m); (E) book-like kaolinite and filamentous illite filled the dissolution pores (LK1, 3482.25 m); (F) book-like kaolinite, filamentous illite, and I/S mixed layer filled the dissolution pores (LK1, 4307.58 m); (G) iron-bearing calcite filled the intergranular dissolution pores (LK1, 4312.03 m); (H) dark organic matter (LK1, 4317.91 m); (I) dark organic matter (LK1, 4433.99 m).

5.3 Control of diagenesis on reservoir properties

For TSR, diagenesis is an important factor causing reservoir densification and strong heterogeneity. Diagenesis can directly change reservoir pore structure and determine the preservation of primary pores and the formation of secondary pores (Li et al., 2005; Wu et al., 2017; Zhang et al., 2021).

5.3.1 Compaction

Among all the types of diagenesis, mechanical compaction is usually the most important factor for pore reduction and mainly affected by burial depth (Lai et al., 2016; Wang et al., 2020; Lv and Li, 2021). Previous studies have shown that mechanical compaction can usually reduce porosity from 45% to 10% at a depth of 4,000 m (Ramm and Bjørlykke, 1994; Hong et al., 2020). According to the CTS observations, the contact between particles is a line, point-line,

and occasionally concave-convex. In addition, the plastic particles (mica, etc.) underwent directional arrangement and extrusion deformation, indicating that the compaction of the LJR was strong. Based on the quantitative calculation above, the initial porosity (Φ_1) of LJR is between 29.6% and 33.3% (avg. 32.2%). According to the relationship between intergranular pore volume (IGV) and cement content first proposed by Houseknecht, 1989, it can be seen that both compaction and cementation lead to the loss of porosity, confirmed by the associated porosity loss rates of 81.5% and 11.8%, respectively. For the LJR, compaction was the most critical factor affecting reservoir densification (Figure 13).

5.3.2 Dissolution

Dissolution significantly enhances the porosity of the TSR (Osborne and Swarbrick, 1999; Hong et al., 2020). According to the CTS observations, dissolution pores have a good relationship with thin section porosity ($R^2 = 0.94$) (Figure 14A), core porosity

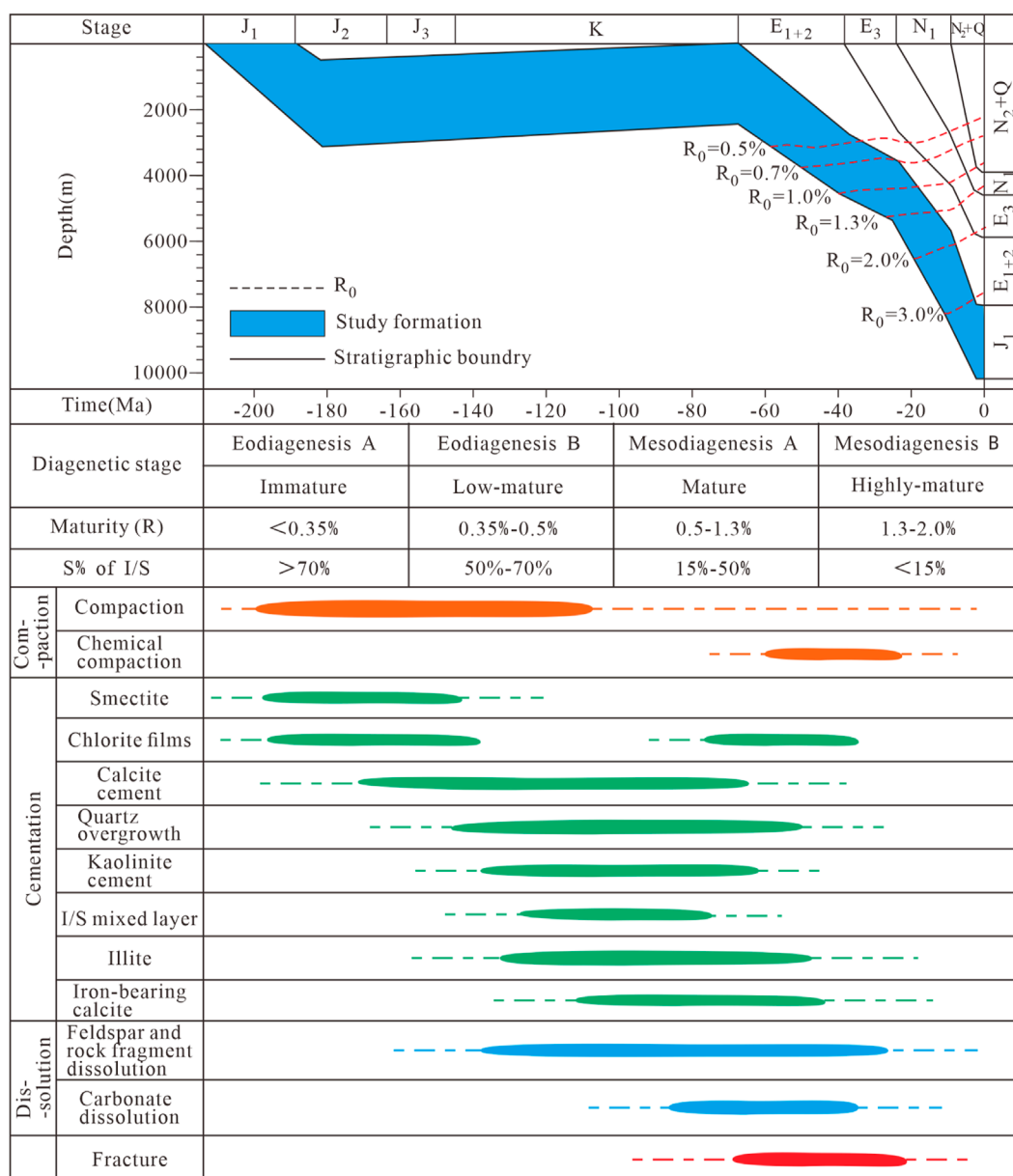


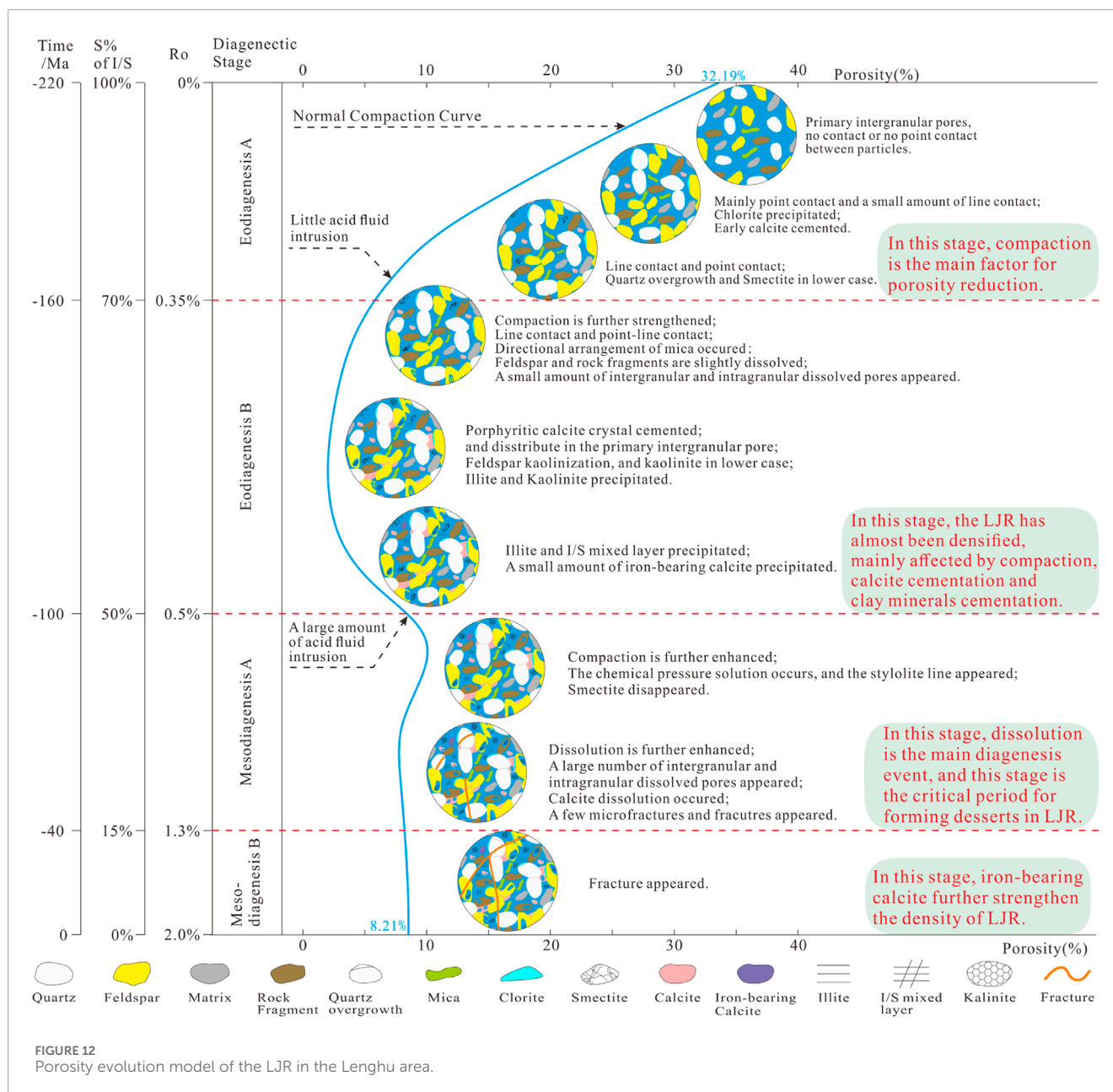
FIGURE 11 Paragenetic sequence in the LJR in the Lenghu area.

($R^2 = 0.55$) (Figure 14B), and core permeability ($R^2 = 0.53$) (Figure 14C). These results indicate that dissolution not only greatly improves the porosity but also improves the permeability of the LJR.

The study area provided suitable conditions for the occurrence of dissolution for the following reasons. Soluble substances (feldspars, rock fragments, calcite cement, etc.) dissolved under the influence of acidic fluids and formed dissolution pores. The rock types in LJR were mainly feldspathic litharenite, litharenite, and lithic arkose. The rock fragments were mainly soluble lithics (such as metamorphic and volcanic lithics). Therefore, the study area had a good material basis for dissolution. Furthermore, many organic acids were released during the maturation of organic matter (Yin et al., 2020). The LJR is a coal-bearing unit, thus its organic acid content is several times that

of general hydrocarbon source rocks (Jiang et al., 2004; Han et al., 2020). Therefore, it provided sufficient organic acids for the early diagenesis of sandstone and laid a material foundation for later dissolution.

According to the cross-plot between the dissolution pores and the burial depth, an apparent dissolution zone developed near 4,400 m (Figure 15A). Thin section observation shows that samples with dissolution pores (black dots) account for 90.6% of the total samples at this depth (Figure 15). Based on the CTS observations, the correlation between dissolution pores and feldspar was poor in this study ($R^2 = 0.12$) (Figure 15B); however, the connection showed an excellent negative correlation at depth of 4,400 m ($R^2 = 0.50$) (Figure 15B). In addition, soluble particles (feldspar, metamorphic



lithics, volcanic lithics, etc.) in all samples had a nil correlation with the dissolution pores, at $R^2 = 0.04$ (Figure 15C). Still, in the dissolution zone, the correlation was moderately good ($R^2 = 0.42$) (Figure 15C). Overall, dissolution in the Lenghu area was dominated by feldspar dissolution, followed by rock fragment dissolution.

5.3.3 Cementation

The cementation of LJR in the Lenghu area was dominated by carbonate and clay mineral cementation. Details are as follows.

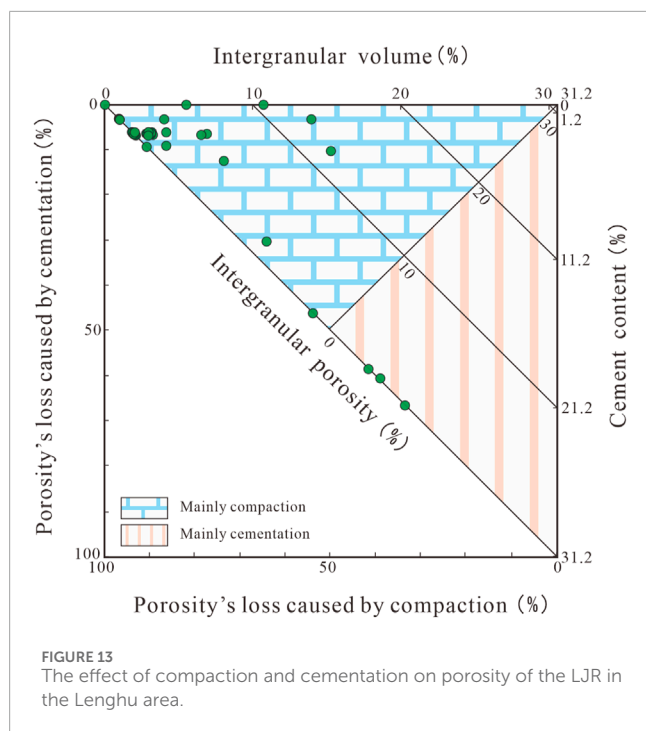
5.3.3.1 Calcite cementation

Based on the CTS observations, the calcite content in the study area had an obvious negative correlation with porosity ($R^2 = 0.70$) (Supplementary Figure S1A), and the correlation between calcite content and permeability was complex. When calcite content is less

than 5%, the correlation between calcite content and permeability is weak; however, when its content exceeded 5%, calcite content and permeability showed a significant negative correlation ($R^2 = 0.63$) (Supplementary Figure S1B). The results show that calcite mainly degrades reservoir properties by filling intergranular or dissolution pores. When the calcite content reaches a certain value (>5%), it significantly affects the reservoir permeability.

5.3.3.2 Clay mineral cementation

The presence of clay minerals is an essential factor affecting the reservoir properties of TSR. Authigenic clay minerals often develop in pores, occupy a certain space, and degrade reservoir properties. As shown in the cross-plot of Supplementary Figure S2, the correlation between reservoir properties (porosity and permeation) and clay mineral content is weak. However, the reservoir properties



show a slightly decreasing trend with the increase of clay mineral content. This means that the clay minerals of LJR have a destructive influence on the reservoir properties, and their effects differ owing to differences in the morphology and composition of the clay minerals. The details are as follows.

Kaolinite was found to be the main clay mineral in the LJR, and the relationship between its content and reservoir properties is complex. When the kaolinite content was less than 40%, it was positively correlated with reservoir properties; however, when it was higher than 40%, porosity and permeability showed a significant negative correlation with kaolinite content. (Supplementary Figures S3A, B). This is because kaolinite often directly fills pores and occupies a certain reservoir space (Worden and Morad, 2003; Li et al., 2017b; Wang et al., 2019). Feldspar dissolution is an important mechanism for kaolinite formation. At the beginning of kaolinite precipitation, the dissolution of feldspar was relatively strong. Kaolinite is too small to crystallize and precipitate *in situ*, so the pore fluid can easily remove it. This process increases the porosity and permeability. Subsequently, feldspar dissolution gradually weakened with the consumption of acidic fluids. At this time, the kaolinite content progressively improved and precipitated *in situ*. During this process, the pores produced by feldspar dissolution were not sufficient to offset the pore loss caused by kaolinite filling, which decreased the porosity and permeability.

I/S mixed-layer content in the study area was slightly lower than that of kaolinite. It mainly developed in the form of filaments and flakes and occupies a certain reservoir space. Filamentous and flaky I/S mixed layers can divide the pore space and decrease reservoir connectivity. The I/S mixed layer content has a moderate correlation with porosity ($R^2 = 0.35$) (Supplementary Figure S3C) and a very correlation with permeability (Supplementary Figure S3D).

Illite content and porosity exhibited a specific positive correlation (Supplementary Figure S3E). This is because a

large amount of K^+ is required for illite formation, most of which originates from the dissolution of potassium feldspar. Simultaneously, the dissolution of potassium feldspar can promote illite formation, and the reaction does not stop until potassium feldspar is completely depleted (Berger et al., 1997). Although the precipitation of illite will occupy a certain pore space, previous studies have demonstrated that during the dissolution of potassium feldspar to form authigenic illite, the overall performance is volume loss and pore space increases, which can create approximately 10.7% of the additional space (Huang et al., 2009). However, filamentous or flake illite increased the curvature of the pores and led to a slight decrease in permeability. Overall, porosity slightly increases with illite content ($R^2 = 0.15$), while permeability slightly decreases ($R^2 = 0.03$) (Supplementary Figures S3E, F).

Chlorite exists in the form of chlorite films. The chlorite film can resist compaction, thus protecting primary pores. In addition, it can inhibit quartz overgrowth (Ajdukiewicz and Larese, 2012; Azzam et al., 2022). Therefore, chlorite content is positively correlated with porosity ($R^2 = 0.60$) (Supplementary Figure S3G). Because it is undeveloped in the LJR, it has little effect on permeability ($R^2 = 0.03$) (Supplementary Figure S3H).

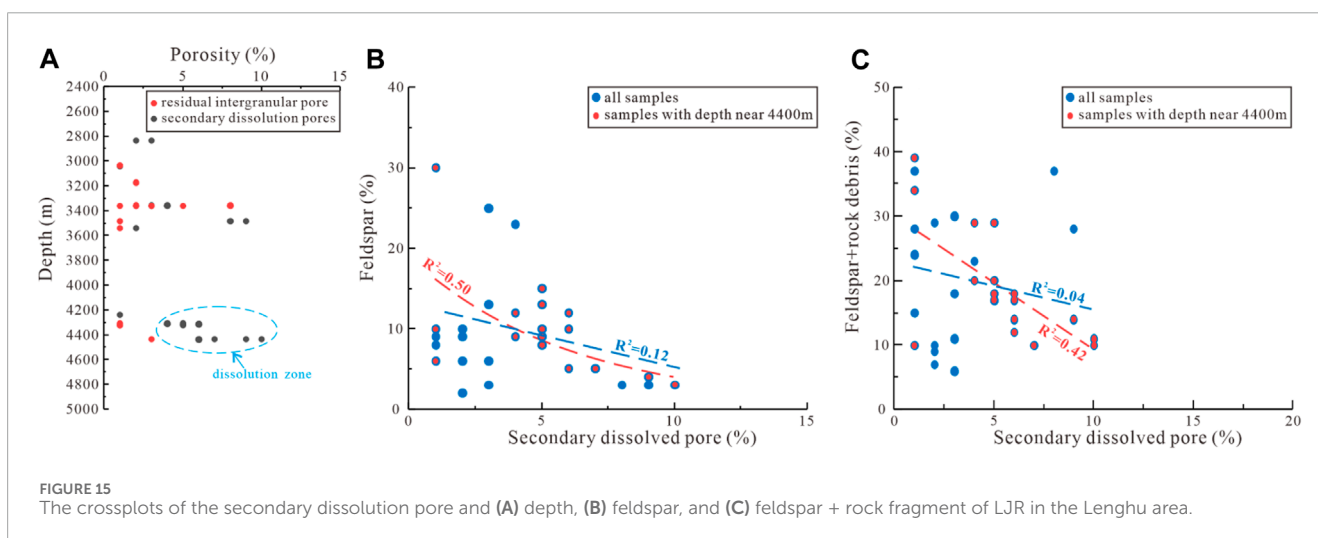
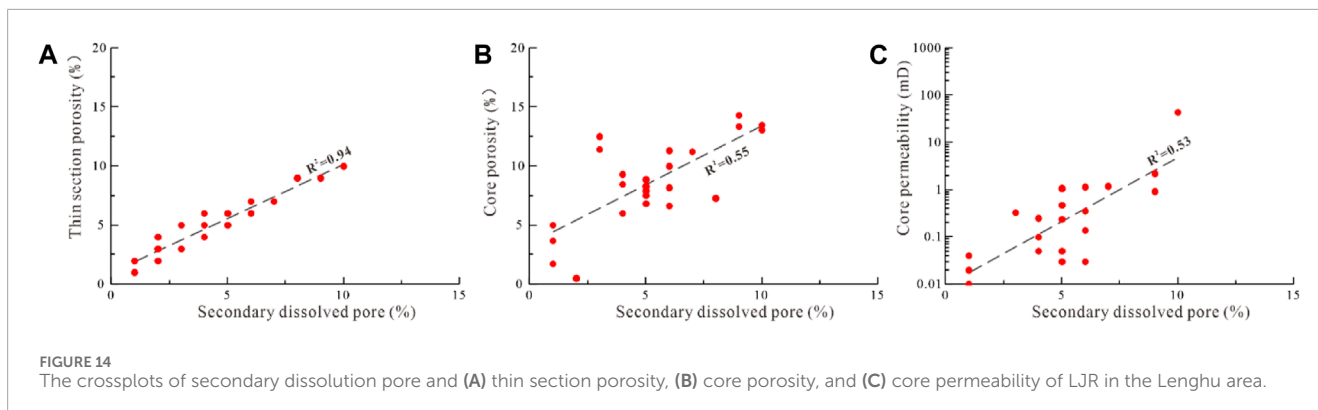
5.4 Reservoir densification mechanism

By establishing a porosity evolution model and quantitative analysis of the influence of different diagenesis on reservoir properties, this study has clarified the densification mechanism of tight sandstone reservoirs in the Lenghu area. The details are as follows:

The initial porosity of unconsolidated sandstone in Lenghu area is 32.2%. In the early stage of diagenesis, diagenesis has little effect on reservoir physical properties. A large number of primary intergranular pores are developed, and compaction is an essential factor in reservoir pore reduction. The reservoir properties are good at this stage, and the tight sandstone reservoir has not yet been formed. In addition, the development of chlorite film is significant for preserving primary pores (Ajdukiewicz and Larese, 2012; Wang et al., 2020). Reservoirs with well-developed chlorite film are favorable zones for developing high quality-reservoir in later stages.

In the eo-diagenetic stage B, the compaction intensity increased gradually as the buried depth increased. At this stage, the porosity loss rate caused by compaction is as high as 81.5%. Additionally, the cementation is also gradually enhanced. Calcite occupied some reservoir space by filling intergranular pores; at the same time, many authigenic clay minerals (such as I/S mixed layer and illite) precipitated and blocked the pore throat system. In this stage, the LJR in the Lenghu area has almost been densified, mainly affected by compaction, calcite cementation and clay minerals cementation.

After entering the meso-diagenetic stage A, the influence of compaction on reservoir properties is relatively weak. Dissolution has become the main diagenetic event in this stage. Soluble particles (such as feldspar, debris and calcite) are dissolved under the action of acidic fluid, thus forming a large number of secondary dissolution pores. The dissolution can significantly improve the reservoir properties. The quantitative calculation above showed that the porosity increased by 6.0% after the dissolution. This stage is the



critical period for forming high quality-reservoir in tight sandstone reservoirs in the Lenghu area, mainly in the 4400 m depth.

In the meso-diagenetic stage B, the influence of dissolution on the reservoir gradually weakened. Although few fractures appeared, they had little effect on reservoir properties. Simultaneously, the cementation of iron-bearing calcite further strengthened the densification of the LJR in the Lenghu area.

6 Conclusion

- The sandstone types of the LJR in the Lenghu area are diverse and are mainly composed of feldspathic litharenite, followed by litharenite and lithic arkose, small amounts of subarkose and sublitharenite. The particles were characterized by line and point-line contact, good-medium sorting, and subangular roundness. The pore types were dominated by secondary dissolution pores, followed by residual intergranular pores and occasional fractures. The LJR is a typical TSR, with average porosity and permeability of 5.5% and 0.08 mD, respectively.
- The LJR has entered the meso-diagenetic stage A, with minor progression into meso-diagenetic stage B. Quantitative estimations suggest shows that the initial porosity of LJR is 32.2%. In the early stage of diagenesis, cementation

and dissolution are weak. Compaction is an important factor for reservoir porosity reduction, and compaction intensity increases with the increase of buried depth. At the eo-diagenetic stage B, the influence of compaction and cementation on porosity reached their peak, and the porosity loss rates were 81.5% and 11.8%, respectively. In this stage, the LJR in the Lenghu area has almost been densified, mainly affected by compaction, calcite cementation and clay minerals cementation. After entering the meso-diagenetic stage A, dissolution is the main diagenesis event, which can increase porosity by 6.0%. In meso-diagenetic stage B, the influence of dissolution gradually decreased, and a small amount of fracturing occurred. Simultaneously, the cementation of iron-bearing calcite further strengthened the densification of the LJR in the Lenghu area.

- Cementation played an important role in the quality and heterogeneity of LJR, and it is dominated by calcite cement. The correlation between porosity and calcite content was very good ($R^2 = 0.7$). Calcite content and permeability showed no obvious correlation when calcite content was <5%; when the calcite content exceeded 5%, it showed a significant negative relationship. Kaolinite is the most abundant clay mineral of LJR. Reservoir properties were positively correlated with kaolinite content when it was <40%, but have a significant

negative correlation when it was higher than 40%. Dissolution can significantly improve reservoir properties, which are mainly developed at 4400 m.

providing research data and samples. We are grateful to the journal editor and reviewers for their comments and suggestions that improved the earlier version of this manuscript.

Data availability statement

The original contributions presented in the study are included in the article/[Supplementary Material](#), further inquiries can be directed to the corresponding author.

Author contributions

WL: Conceptualization, Data curation, Formal Analysis, Investigation, Methodology, Project administration, Software, Validation, Visualization, Writing—original draft, Writing—review and editing. DH: Conceptualization, Formal Analysis, Funding acquisition, Investigation, Methodology, Project administration, Supervision, Visualization, Writing—original draft, Writing—review and editing. YC: Conceptualization, Formal Analysis, Funding acquisition, Methodology, Project administration, Supervision, Writing—review and editing. YL: Funding acquisition, Investigation, Methodology, Resources, Software, Validation, Visualization, Writing—review and editing. BG: Data curation, Software, Visualization, Writing—review and editing, Resources. QS: Investigation, Resources, Software, Validation, Writing—review and editing. BZ: Data curation, Software, Writing—review and editing.

Funding

The author(s) declare financial support was received for the research, authorship, and/or publication of this article. This study was jointly supported by the project from the Research Institute of Exploration and Development of Qinghai Oilfield (Grant 2018-Technique-Exploration-02) and the PetroChina prospective basic strategic technology research project (Grant 2022DJ3209). The funders were not involved in the study design, collection, analysis, interpretation of data, the writing of this article, or the decision to submit it for publication.

Acknowledgments

We sincerely thank the Research Institute of Exploration and Development of Qinghai Oilfield Company, PetroChina, for

References

- Ajdkiewicz, J. M., and Larese, R. E. (2012). How clay grain coats inhibit quartz cement and preserve porosity in deeply buried sandstones: observations and experiments. *AAPG Bull.* 96 (11), 2091–2119. doi:10.1306/02211211075
- Azzam, F., Blaise, T., Patrier, P., Abd Elmola, A., Beaufort, D., Portier, E., et al. (2022). Diagenesis and reservoir quality evolution of the Lower Cretaceous turbidite sandstones of the Agat Formation (Norwegian North Sea): impact of clay grain coating and carbonate cement. *Mar. Petroleum Geol.* 142, 105768. doi:10.1016/j.marpetgeo.2022.105768
- Beard, D. C., and Weyl, P. K. (1973). Influence of texture on porosity and permeability of unconsolidated sand. *AAPG Bull.* 57 (2), 349–369. doi:10.1306/819A4272-16C5-11D7-8645000102C1865D
- Berger, G., Lachapagne, J. C., Velde, B., Beaufort, D., and Lanson, B. (1997). Kinetic constraints on illitization reactions and the effects of organic diagenesis in sandstone/shale sequences. *Appl. Geochemistry* 12 (1), 23–35. doi:10.1016/S0883-2927(96)00051-0
- Cao, B. F., Sun, W., and Li, J. (2020). Reservoir petrofacies - a tool for characterization of reservoir quality and pore structures in a tight sandstone reservoir: a study from the

Conflict of interest

Authors WL, DH and YC were employed by the Research Institute of Petroleum Exploration and Development PetroChina. Authors YL and QS were employed by the Research Institute of Exploration and Development of Qinghai Oilfield Company. Author BG was employed by the New Energy Department of Qinghai Oilfield Company. Author BZ was employed by the Zhongyuan Oilfield Company.

The remaining authors declare that the research was conducted in the absence of any commercial or financial relationships that could be construed as a potential conflict of interest.

Publisher's note

All claims expressed in this article are solely those of the authors and do not necessarily represent those of their affiliated organizations, or those of the publisher, the editors and the reviewers. Any product that may be evaluated in this article, or claim that may be made by its manufacturer, is not guaranteed or endorsed by the publisher.

Supplementary material

The Supplementary Material for this article can be found online at: <https://www.frontiersin.org/articles/10.3389/feart.2024.1298802/full#supplementary-material>

SUPPLEMENTARY FIGURE S1

The crossplots of the calcite content and (A) porosity, (B) permeability of LJR in the Lenghu area.

SUPPLEMENTARY FIGURE S2

The crossplots of clay minerals content and (A) porosity, (B) permeability of LJR in the Lenghu area.

SUPPLEMENTARY FIGURE S3

The relationships between clay minerals and reservoir properties of LJR in the Lenghu area: kaolinite with (A) porosity and (B) permeability; I/S mixed layer with (C) porosity and (D) permeability; illite with (E) porosity and (F) permeability; chlorite with (G) porosity and (H) permeability.

- sixth member of Upper Triassic Yanchang Formation, Ordos Basin, China. *J. Petroleum Sci. Eng.* 199, 108294. doi:10.1016/j.petrol.2020.108294
- Cao, Z. L., Sun, X. J., Wu, W. J., Tian, G. R., Zhang, S. M., Li, H. B., et al. (2018). Formation and evolution of thrust paleo-uplift at the margin of Qaidam Basin and its influence on hydrocarbon accumulation. *Acta Pet. Sin.* 39 (9), 980–989. doi:10.19901/j.fcgyq.2021.01.07
- Dai, B., Wen, H. Y., Ren, Z. Y., Wang, L. F., Kang, L. H., Yang, X. Y., et al. (2021). Microscopic pore characteristics and main controlling factors of Chang 7 tight sandstone in Ansai Oilfield. *Unconv. Oil Gas* 8 (01), 51–59. doi:10.19901/j.fcgyq.2021.01.07
- Dai, J. X., Ni, Y. Y., and Wu, X. Q. (2012). Tight gas in China and its significance in exploration and exploitation. *Petroleum Explor. Dev.* 39 (3), 277–284. doi:10.1016/S1876-3804(12)60043-3
- Fang, X. X., Guo, Y. C., Wang, P., Wang, P. W., and Guo, J. G. (2020). The progress of research on tight oil accumulation and several scientific issues requiring further study. *Geol. China* 47 (1), 43–56. doi:10.1029/gc20200104
- Folk, R. L. *Petrology of Sedimentary Rocks*; Hemphill Publishing Company: Austin, TX, USA, 1980; p. 182.
- Fu, S. T., Zhang, D. W., Xue, J. Q., and Zhang, X. B. (2013). Exploration potential and geological conditions of tight oil in the Qaidam Basin. *Acta Sedimentol. Sin.* 31 (04), 672–682. doi:10.14027/j.cnki.cjxb.2013.04.011
- Guo, J. J., Sun, G. Q., Long, G. H., Guan, B., Kang, J., Xia, W. M., et al. (2017). Sedimentary diagenesis environment of the lower jurassic in Lenghu Tectonic Belt, Northern Qaidam Basin. *Nat. Gas. Geosci.* 107, 149–162. doi:10.11764/j.issn.1672-1926.2017.11.006
- Guo, P., Liu, C. Y., Wang, L. Q., Zhang, G. Q., and Fu, X. G. (2019). Mineralogy and organic geochemistry of the terrestrial lacustrine pre-salt sediments in the Qaidam Basin: implications for good source rock development. *Mar. Petroleum Geol.* 107, 149–162. doi:10.1016/j.marpetgeo.2019.04.029
- Guo, Y. C., Cao, J., Liu, R. Q., Wang, H. F., and Zhang, H. Y. (2022). Hydrocarbon accumulation and alteration of the upper carboniferous keluke Formation in the eastern Qaidam Basin: insights from fluid inclusion and basin modeling. *J. Petroleum Sci. Eng.* 211, 110116. doi:10.1016/j.petrol.2022.110116
- Guo, Y. C., Pang, X. Q., Chen, D. X., and Zhu, H. Q. (2012). Densification of tight gas sandstones and formation mechanism of relatively high-quality reservoir in the second member of the xujiahe formation, western sichuan depression. *J. Jilin Univ. Earth Sci. Ed.* 42 (S2), 21–32. doi:10.13278/j.cnki.jiuese.2012.s2.003
- Han, Y., Gao, X. Z., Zhou, F., Wang, B., Zhu, J., and Duan, L. F. (2020). Thermal evolution of Jurassic source rocks and their impact on hydrocarbon accumulation in the northern margin of Qaidam Basin, NW China. *Geoscience* 31 (3), 358–369.
- He, W. A., Barzgar, E., Feng, W. P., and Huang, L. (2021). Reservoirs patterns and key controlling factors of the Lenghu oil & gas field in the Qaidam Basin, northwestern China. *J. Earth Sci.* 32 (4), 1011–1021. doi:10.1007/s12583-020-1061-z
- Hong, D. D., Cao, J., Wu, T., Dang, S. S., Hu, W. X., and Yao, S. P. (2020). Authigenic clay minerals and calcite dissolution influence reservoir quality in tight sandstones: insights from the central Junggar Basin, NW China. *Energy Geosci.* 1 (1–2), 8–19. doi:10.1016/j.engeos.2020.03.001
- Hou, H. H., Shao, L. Y., Li, Y. H., Liu, L., Liang, G. D., Zhang, W. L., et al. (2022). Effect of paleoclimate and paleoenvironment on organic matter accumulation in lacustrine shale: constraints from lithofacies and element geochemistry in the northern Qaidam Basin, NW China. *J. Petroleum Sci. Eng.* 208, 109350. doi:10.1016/j.petrol.2021.109350
- Houseknecht, D. W. (1989). Assessing the relative importance of compaction processes and cementation to reduction of porosity in sandstones: reply. *AAPG Bull.* 73 (10), 1277–1279. doi:10.1306/44b4aa23-170a-11d7-8645000102c1865d
- Huang, S. J., Huang, K. K., Feng, W. L., Tong, H. P., Liu, L. H., and Zhang, X. H. (2009). Mass exchanges among feldspar, kaolinite and illite and their influences on secondary porosity formation in clastic diagenesis: A case study on the Upper Paleozoic, Ordos Basin and Xujiahe Formation, Western Sichuan Depression. *Geochimica* 38 (5), 498–506. doi:10.19790/j.0379-1726.2009.05.009
- Jia, C. Z. (2017). Breakthrough and significance of unconventional oil and gas to classical petroleum geology theory. *Petroleum Explor. Dev.* 44 (1), 1–10. doi:10.1016/S1876-3804(17)30002-2
- Jiang, L. Z., Gu, J. Y., and Guo, B. C. (2004). Characteristics and mechanism of low permeability clastic reservoir in Chinese petroliferous basin. *Acta Sedimentol. Sin.* 22 (1), 13–18. doi:10.3969/j.issn.1000-0550.2004.01.003
- Ju, W., and Wang, K. (2018). A preliminary study of the present-day *in-situ* stress state in the Ahe tight gas reservoir, Dibe Gasfield, Kuqa Depression. *Mar. Petroleum Geol.* 96, 154–165. doi:10.1016/j.marpetgeo.2018.05.036
- Karim, A., Piper, P. G., and Piper, J. M. D. (2010). Controls on diagenesis of lower cretaceous reservoir sandstones in the western sable subbasin, offshore nova scotia. *Sediment. Geol.* 224 (1–4), 65–83. doi:10.1016/j.sedgeo.2009.12.010
- Lai, J., Wang, G. W., Ran, Y., Zhou, Z. L., and Cui, Y. F. (2016). Impact of diagenesis on the reservoir quality of tight oil sandstones: the case of Upper Triassic Yanchang Formation Chang 7 oil layers in Ordos Basin, China. *J. Petroleum Sci. Eng.* 145, 54–65. doi:10.1016/j.petrol.2016.03.009
- Law, B. E., and Curtis, J. B. (2002). Introduction to unconventional petroleum systems. *AAPG* 86 (11), 1851–1852. doi:10.1306/61eedda0-173e-11d7-8645000102c1865d
- Li, J., Luo, X., Shan, X. Q., Ma, C., Hu, G., Yan, Q., et al. (2005). Natural gas accumulation in the upper paleozoic of Ordos Basin, China. *Petroleum Explor. Dev.* 32 (4), 54–59. doi:10.3321/j.issn:1000-0747.2005.04.009
- Li, J., Tian, J. X., Liu, C. L., Feng, D. H., Zeng, X., Zhang, M., et al. (2021). Geochemical characteristics and source analysis of natural gas in the saline lacustrine basin in the Western Qaidam basin. *J. Petroleum Sci. Eng.* 201, 108363. doi:10.1016/j.petrol.2021.108363
- Li, Y., Chang, X. C., Yin, W., Sun, T. T., and Song, T. T. (2017a). Quantitative impact of diagenesis on reservoir quality of the Triassic Chang 6 tight oil sandstones, Zhenjing area, Ordos Basin, China. *Mar. Petroleum Geol.* 86, 1014–1028. doi:10.1016/j.marpetgeo.2017.07.005
- Li, Y., Fan, A. P., Yang, R. C., Sun, Y. P., and Lenhardt, N. (2021). Sedimentary facies control on sandstone reservoir properties: a case study from the permian Shanxi Formation in the southern Ordos basin, central China. *Mar. Petroleum Geol.* 129, 105083. doi:10.1016/j.marpetgeo.2021.105083
- Li, Y., Li, S. T., Mou, W. W., and Yan, C. C. (2017b). Influences of clay minerals on physical properties of Chang 6 tight sandstone reservoir in Jiyuan area, Ordos Basin. *Nat. Gas. Geosci.* 28 (7), 1043–1053. doi:10.11764/j.issn.1672-1926.2017.06.015
- Liu, F., Wang, X., Liu, Z. B., Tian, F., Zhao, Y. W., Pan, G. H., et al. (2023). Identification of tight sandstone reservoir lithofacies based on CNN image recognition technology: a case study of Fuyu reservoir of Sanzhao Sag in Songliao Basin. *Geoenery Sci. Eng.* 222, 211459. doi:10.1016/j.geoen.2023.211459
- Liu, K., Wang, R., Shi, W. Z., Trave, A., Martin-Martin, J. D., Baques, V., et al. (2022). Diagenetic controls on reservoir quality and heterogeneity of the Triassic Chang 8 tight sandstones in the Binchang area (Ordos Basin, China). *Mar. Petroleum Geol.* 146, 105974. doi:10.1016/j.marpetgeo.2022.105974
- Liu, Z. G., Si, C. S., Shou, J. F., N. C., Pan, L. Y., and Liu, Q. (2011). Origin mechanism of anomalous tightness of middle and lower jurassic sandstone reservoirs in central sichuan basin. *Acta Sedimentol. Sin.* 29 (4), 744–751. doi:10.14027/j.cnki.cjxb.2011.04.012
- Lv, T. X., and Li, Z. P. (2021). Quantitative characterization method for microscopic heterogeneity in tight sandstone. *Energy Explor. Exploitation* 39 (4), 1076–1096. doi:10.1177/0144598721993937
- Ma, D. D., Yuan, L., Chen, Y., Zhou, F., Wu, Z. X., Lei, T., et al. (2018). Geological conditions of natural gas, resource potential and exploration direction in the northern margin of Qaidam Basin. *Nat. Gas. Geosci.* 29 (10), 1486–1496. doi:10.11764/j.issn.1672-1926.2018.09.009
- Mao, L. G., Xiao, A. C., Zhang, H. W., Wu, Z. K., Wang, L. Q., Shen, Y., et al. (2016). Structural deformation pattern within the NW Qaidam Basin in the Cenozoic era and its tectonic implications. *Tectonophysics* 687, 78–93. doi:10.1016/j.tecto.2016.09.008
- Osborne, M. J., and Swarbrick, R. E. (1999). Diagenesis in North sea HPHT clastic reservoirs consequences for porosity and overpressure prediction. *Mar. Petroleum Geol.* 16 (4), 337–353. doi:10.1016/S0264-8172(98)00043-9
- Pang, Y. M., Zou, K. Z., Guo, X. W., Chen, Y., Zhao, J., Zhou, F., et al. (2022). Geothermal regime and implications for basin resource exploration in the Qaidam Basin, northern Tibetan Plateau. *J. Asian Earth Sci.* 239, 105400. doi:10.1016/j.jseas.2022.105400
- Qin, S., Wang, R., Shi, W. Z., Liu, K., Zhang, W., Xu, X. F., et al. (2022). Diverse effects of intragranular fractures on reservoir properties, diagenesis, and gas migration: insight from Permian tight sandstone in the Hangjinqi area, north Ordos Basin. *Mar. Petroleum Geol.* 137, 105526. doi:10.1016/j.marpetgeo.2022.105526
- Ramm, M., and Bjorlykke, K. (1994). Porosity/depth trends in reservoir sandstones: assessing the quantitative effects of varying pore-pressure, temperature history and mineralogy, Norwegian shelf data. *Clay Miner.* 29 (4), 475–490. doi:10.1180/claymin.1994.029.4.07
- Ritts, B. D., Hanson, A. D., Zinniker, D., and Moldowan, J. M. (1999). Lower–Middle Jurassic nonmarine source rocks and petroleum systems of the northern Qaidam basin, northwest China. *AAPG Bull.* 83 (12), 1980–2005. doi:10.1306/E4FD4661-1732-11D7-8645000102C1865D
- Su, N. N., Song, F., Qiu, L. W., and Zhang, W. (2021). Diagenetic evolution and densification mechanism of the upper paleozoic tight sandstones in the Ordos basin, northern China. *J. Asian Earth Sci.* 205, 104613. doi:10.1016/j.jseas.2020.104613
- Sun, D. Q., Liu, H. T., Yu, H. L., Liu, J. C., and Zhang, T. (2006). Mechanisms of petroleum accumulation of structural reservoir in No. 5 Unit of Lenghu area in Qaidam Basin. *Xinjiang Pet. Geol.* 27 (4), 435–439.
- Sun, G. Q., Si, D., Wang, M., Shen, Y. S., Zhou, F., Hao, X. M., et al. (2012). The tectonic kinematic process and the types of oil and gas reservoirs in northern margin of Qaidam Basin. *Nat. Gas. Geosci.* 23 (5), 826–832.
- Sun, L. D., Zou, C. N., Jia, A. L., Wei, Y. S., Zhu, R. K., Wu, S. T., et al. (2019). Development characteristics and orientation of tight oil and gas in China. *Petroleum Explor. Dev.* 46 (9), 1073–1087. doi:10.1016/S1876-3804(19)60264-8
- Tang, L. J., Jin, Z. J., Zhang, M. L., Liu, C. Y., Wu, H. N., You, F. B., et al. (2000). Structural paleogeographic analysis of Qaidam Basin. *Earth Sci. Front.* 7 (4), 421.

- Tian, J. X., Ji, B. Q., Zeng, X., Wang, Y. T., Li, Y. L., and Sun, G. Q. (2022). Development characteristics and main controlling factors of deep clastic reservoir of the Xiaganchaigou Formation in the northern margin of Qaidam Basin, China. *Nat. Gas. Geosci.* 33 (5), 720–730. doi:10.11764/j.issn.1672-1926.2021.07.011
- Tian, J. X., Li, J., Pan, C. F., Tan, Z., Zeng, X., Guo, Z. Q., et al. (2018). Geochemical characteristics and factors controlling natural gas accumulation in the northern margin of the Qaidam Basin. *J. Petroleum Sci. Eng.* 160, 219–228. doi:10.1016/j.petrol.2017.10.065
- Wang, E. Z., Pang, X. Q., Zhao, X. D., Wang, Z. J., Wang, Z. M., H. T., et al. (2020). Characteristics, diagenetic evolution, and controlling factors of the Es1 deep burial high-quality sandstone reservoirs in the PG2 oilfield, Nanpu Sag, Bohai Bay Basin, China. *Geol. J.* 55 (4), 2403–2419. doi:10.1002/gj.3507
- Wang, W. R., Yue, D. L., Zhao, J. Y., Li, W., Wang, B., Wu, S. H., et al. (2019). Diagenetic alteration and its control on reservoir quality of tight sandstones in lacustrine deepwater gravity-flow deposits: a case study of the Yanchang Formation, southern Ordos Basin, China. *Mar. Petroleum Geol.* 110, 676–694. doi:10.1016/j.marpetgeo.2019.07.046
- Wang, Y. N., Lin, L. B., Yu, Y., Li, Y. H., Guo, Y., and Deng, X. L. (2019). Characteristics of kaolinite in tight sand reservoirs of Member 4 of Upper Triassic Xujiahe Formation in west Sichuan depression and its influence on physical properties of reservoirs. *J. Chengdu Univ. Technol.* 46 (3), 354–362. doi:10.3969/j.issn.1671-9727.2019.03.10
- Wang, Z. N., Luo, X. R., Lei, Y. H., Zhang, L. K., Shi, H., Lu, J. H., et al. (2020). Impact of detrital composition and diagenesis on the heterogeneity and quality of low-permeability to tight sandstone reservoirs: an example of the Upper Triassic Yanchang Formation in Southeastern Ordos Basin. *J. Petroleum Sci. Eng.* 195, 107596. doi:10.1016/j.petrol.2020.107596
- Worden, R. H., and Morad, S. (2003). *Clay minerals in sandstones: controls on formation*. Oxford: Distribution and Evolution. doi:10.1002/9781444304336.ch1
- Wu, D., Li, H., Jiang, L., Hu, S. H., Wang, Y. H., Zhang, Y. L., et al. (2019). Diagenesis and reservoir quality in tight gas bearing sandstones of a tidally influenced fan delta deposit: the Oligocene Zhuhai Formation, western Pearl River Mouth Basin, South China Sea. *Mar. Petroleum Geol.* 107, 278–300. doi:10.1016/j.marpetgeo.2019.05.028
- Wu, H., Ji, Y., Liu, R., Zhang, C., and Chen, S. (2017). Insight into the pore structure of tight gas sandstones: a case study in the Ordos Basin, NW China. *Energy Fuels* 31 (12), 13159–13178. doi:10.1021/acs.energyfuels.7b01816
- Wu, X. Z., Liuzhuang, X. X., Wang, J., Zheng, M., Chen, X. M., and Qi, X. F. (2022). Petroleum resource potential, distribution and key exploration fields in China. *Earth Sci. Front.* 29 (6), 146–155. doi:10.13745/j.esf.sf.2022.8.27
- Xi, K. L., Cao, Y. C., Jahren, J., Zhu, R. K., Bjørlykke, K., Haile, B. G., et al. (2015). Diagenesis and reservoir quality of the lower cretaceous Quantou formation tight sandstones in the southern Songliao Basin, China. *Sediment. Geol.* 330, 90–107. doi:10.1016/j.sedgeo.2015.10.007
- Xiao, X. X., Qin, L. Z., Zhang, W., Jiang, X., and Zhang, C. (2023). Reservoir characteristics and densification process of Pinghu Formation in western slope of Xihu Sag. *Margine Geol. Front.* 39 (4), 34–35. doi:10.16028/j.1009-2722.2022.023
- Xu, H., Liu, M. J., Zhang, Z., Ye, S. J., Yang, Y. T., Wu, L., et al. (2022). Diagenesis and porosity evolution of the 3-(rd) member of xujiahe formation tight sandstone reservoir in the western sichuan Depression, Sichuan basin. *Nat. Gas. Geosci.* 33 (3), 344–357. doi:10.11764/j.issn.1672-1926.2021.10.007
- Xu, W., Bao, J. P., Liu, T., and Yin, X. (2008). Evaluation on hydrocarbon source rock of lower jurassic, Lenghu area. Northern margin of Qaidam Basin. *Nat. Gas. Geosci.* 19 (5), 707–712.
- Yin, S., Dong, L., Yang, X., and Wang, R. Y. (2020). Experimental investigation of the petrophysical properties, minerals, elements and pore structures in tight sandstones. *J. Nat. Gas Sci. Eng.* 76, 103189. doi:10.1016/j.jngse.2020.103189
- Yuan, G. H., Gluyas, J., Cao, Y. C., Oxtoby, N. H., Jia, Z. Z., Wang, Y. Z., et al. (2015). Diagenesis and reservoir quality evolution of the eocene sandstones in the northern dongying sag, Bohai bay basin, east China. *Mar. Petroleum Geol.* 62, 77–89. doi:10.1016/j.marpetgeo.2015.01.006
- Zhai, Z. W., Zhang, Y. S., Yang, H. M., Sha, W., Nian, X. Q., Hao, X. M., et al. (2013). Characteristics of effective source rocks in the Jurassic and hydrocarbon accumulation patterns in the areas near the northern margin of the Qaidam Basin. *Nat. Gas. Ind.* 33 (9), 36–42. doi:10.3787/j.issn.1000-0976.2013.09.006
- Zhang, C., Wang, S. B., Yu, R. A., Cheng, Y. H., Tu, J. R., Ao, C., et al. (2022). Occurrence of uranium minerals in the Xiaomeigou Formation in northern Qaidam Basin, northwest China. *Ore Geol. Rev.* 142, 104692. doi:10.1016/j.oregeorev.2021.104692
- Zhang, R. H., Yang, H. J., Wang, J. P., Shou, J. F., Zeng, Q. L., and Liu, Q. (2014). The formation mechanism and exploration significant of ultra-deep, low-porosity and tight sandstone reservoirs in Kuqa depression, Tarim Basin. *Acta Pet. Sin.* 35 (6), 1057–1069. doi:10.7623/syxb201406003
- Zhang, S. N. (2008). Tight sandstone gas reservoirs: their origin and discussion. *Oil Gas Geol.* 29 (1), 1–10.
- Zhang, Y. Y., Jiang, S., He, Z. L., Wang, Y. B., Guo, M. Q., Zhu, G. H., et al. (2021). Characteristics of heterogeneous diagenesis and modification to physical properties of Upper Paleozoic tight gas reservoir in eastern Ordos Basin. *J. Petroleum Sci. Eng.* 28, 109243. doi:10.1016/j.petrol.2021.109243
- Zhang, Z. G., Yuan, J. Y., Yan, C. F., and Ma, X. M. (2009). Controlling factors of hydrocarbon accumulation of Lenghu No. 3–5 structural belt in northern Qaidam Basin. *Lithol. Reserv.* 21 (2), 42–44.
- Zhao, J. F., Zeng, X., Tian, J. X., Hu, C., Wang, D., Yan, Z. D., et al. (2020). Provenance and paleogeography of the Jurassic Northwestern Qaidam Basin (NW China): evidence from sedimentary records and detrital zircon geochronology. *J. Asian Earth Sci.* 190, 104060. doi:10.1016/j.jseaes.2019.104060
- Zhou, F., Wang, B., Li, Z. X., Sui, G. J., Qi, W. Z., Cui, S. K., et al. (2019). Geochemical characteristics and accumulation elements controlling the natural gas in Lenghu tectonic belts of Qaidam Basin. *Nat. Gas. Geosci.* 30 (10), 1496–1507. doi:10.11746/j.issn.1672-1926.06.003
- Zhu, P., Meng, X. H., Wang, X., Dong, Y. X., Li, X. W., Zhang, C. H., et al. (2022). Geochemical characteristics of diagenetic fluid and densification model of tight gas sandstone reservoirs in Linxing area, eastern margin of Ordos Basin, China. *Mar. Petroleum Geol.* 239, 105496. doi:10.1016/j.marpetgeo.2021.105496
- Zhu, S. F., Taylor, K., Chen, J. H., Zhu, X. M., Sun, S. Y., and Jia, Y. (2019). Controls on carbonate cementation in early syn-rift terrestrial siliciclastics: the Lower Cretaceous of the Bayindulan Sag in Er'lian Basin, China. *Mar. Petroleum Geol.* 105, 64–80. doi:10.1016/j.marpetgeo.2019.04.013
- Zhu, X. M., Pan, R., Zhu, S. F., Wei, W., and Ye, L. (2018). Research progress and core issues in tight reservoir exploration. *Earth Sci. Front.* 25 (2), 141–146. doi:10.13745/j.esf.2018.02.015
- Zhuo, X. Z., Zhang, L. Y., Chen, X. S., Zhang, J. J., Yang, J. L., and Li, Y. C. (2015). Influence of the argillaceous matrix on pore evolution model of the deep reservoir in well kun-2, Qaidam Basin. *Geol. Rev.* 61 (6), 1447–1457. doi:10.11746/j.issn.1672-1926.06.003
- Zou, C. N., Zhang, G. Y., Tao, S. Z., Hu, S. Y., Li, X. D., Li, J. Z., et al. (2010). Geological features, major discoveries and unconventional petroleum geology in the global petroleum exploration. *Petroleum Explor. Dev.* 37 (2), 129–145. doi:10.1016/s1876-3804(10)60021-3
- Zou, C. N., Zhu, R. K., Wu, S. T., Yang, Z., Tao, S. Z., Yuan, X. J., et al. (2012). Types, characteristics, genesis and prospects of conventional and unconventional hydrocarbon accumulations: taking tight oil and tight gas in China as an instance. *Acta Pet. Sin.* 33 (2), 173–187. doi:10.7623/syxb201202001